SLAP controls mTORC2 integrity via UBE3C-mediated non-degradative mLST8 ubiquitination to suppress colorectal tumorigenesis

Rudy Mevizou, Dana Naim, Florent Cauchois, Cécile Naudin, Georgia Greaves, Kevin Espie, Bastien Felipe, Valérie Simon, Yvan Boublik, Julie Nguyen, et al.

CDDpress

www.nature.com/cdd

ARTICLE OPEN

Check for updates

SLAP controls mTORC2 integrity via UBE3C-mediated non-degradative mLST8 ubiquitination to suppress colorectal tumorigenesis

Rudy Mevizou[1,2,5], Dana Naim[1,2,3,5], Florent Cauchois[1,3], Cécile Naudin[1], Georgia Greaves[1], Kevin Espie[1], Bastien Felipe[1], Valérie Simon[1,2], Yvan BOUBLIK[1,2,3], Julie Nguyen[1,2,3], Serge Urbach[4], Serge Roche[1,2,3,5]✉ and Audrey Sirvent[1,2,3,5]✉

The mechanistic target of rapamycin complex 2 (mTORC2) signaling pathway, which regulates cell growth and migration, exhibits oncogenic function in colorectal cancer (CRC). mTORC2 signaling is primarily activated by a complex assembly of mTOR, RICTOR, SIN1, and mLST8; however, the mechanisms by which dysregulation of this pathway contributes to its oncogenic function remain elusive. Here, we show that the Src-Like Adaptor Protein (SLAP), a negative regulator of tyrosine kinase signaling receptors, controls mTORC2 integrity to mediate its tumor-suppressive function in CRC. Mechanistically, SLAP interacts with mLST8 and facilitates its non-degradative ubiquitination at lysines 86 and 215, thereby reducing the integrity of mTORC2 and mTORC2-AKT signaling. The E3 ubiquitin ligase UBE3C was identified as a novel SLAP interactor involved in this ubiquitination process. Functionally, SLAP inhibition of CRC cell growth and invasion was dependent upon mTORC2 signaling inhibition. In immunodeficient mice CRC xenografts, SLAP depletion enhanced mTORC2 activity and sensitized CRC cells to mTOR catalytic inhibitors. Together, our findings reveal a previously unrecognized SLAP–UBE3C–mLST8 axis that regulates mTORC2 integrity and suggest a potential therapeutic avenue for targeting mTORC2 in CRC.

Cell Death & Differentiation; https://doi.org/10.1038/s41418-025-01633-1

INTRODUCTION

The mechanistic target of rapamycin (mTOR) is a key regulator of eukaryotic cell growth and metabolism induced by growth factors and nutrient availability [1, 2]. mTOR is a serine/threonine protein of the phosphoinositide 3-kinase (PI3K)-related protein kinases (PIKK) family that mediates its cellular functions through two distinct complexes, mTOR complex 1 (mTORC1) and mTOR complex 2 (mTORC2) [1, 2]. mTOR and mLST8 are core components of both complexes, while RAPTOR is a specific constituent of mTORC1 and SIN1 and RICTOR of mTORC2. mTORC1 primarily controls protein synthesis and anabolic metabolism, whereas mTORC2 is involved in cell survival, proliferation and cytoskeletal dynamics [1, 2]. Although the regulation of mTORC1 has been extensively studied, much less is known about the regulation of mTORC2 [1, 3]. It is well established that mTORC2 is activated by a PI3K-dependent growth factor receptor signaling and mediates its cellular function by activating AGC (PKA, PKC and PKG) protein kinases, in particular by phosphorylating AKT at Ser473 to activate cell survival and migration [1, 3]. mTORC2 activity is frequently dysregulated in human cancers, particularly in colorectal cancer (CRC), where it plays an important oncogenic role [4–7]. Notably, mTORC2 overactivation is involved in CRC cell proliferation, dissemination and therapeutic resistance [4, 5, 7, 8]. Consequently, mTORC2 has been defined as an attractive therapeutic target in CRC. However, developed mTOR inhibitors have shown variable efficacy in CRC due to a lack of specificity or induction of resistance mechanisms that overcome mTOR kinase inhibition [9–12]. Deciphering the underlying mechanism of mTORC2 oncogenic activation may lead to more effective mTORC2-based therapy.

mTORC2 signaling is primarily activated by complex assembly [1, 13]. Ubiquitination has emerged as a key regulatory mechanism of this molecular process. For example, the co-chaperone TELO2-TTI1-TTI2 (TTT) complex defines a key control mechanism for the stabilization of PIKKs during translation, including mTORC2 [3, 13]. Its degradation by the ubiquitin ligase SCFFbxo9 has been reported to regulate mTORC2 abundance and survival AKT signaling in multiple myeloma [14]. Similarly, specific mTORC2 components (e.g., RICTOR and mTOR) have been subjected to ubiquitination-dependent degradation, affecting complex integrity and signaling [6, 15]. Interestingly, recent findings have uncovered a non-degradative ubiquitylation mechanism of mTORC2 disassembly, via inhibition of the specific scaffolding function of mLST8 in this complex. mLST8 ubiquitination on Ub-K63, is mediated by TRAF2 and is overridden by the growth factor-responsive deubiquitinase OTUD7B [16]. A similar mechanism has been reported for RICTOR via the deubiquitinase USP9X [17], suggesting a central mechanism of mTORC2 regulation. However,

[1]CRBM, Université de Montpellier, CNRS, Montpellier, France. [2]Equipe labellisée LIGUE, CRBM, Université de Montpellier, CNRS, Montpellier, France. [3]Equipe labellisée FRM, CRBM, Université de Montpellier, CNRS, Montpellier, France. [4]IGF, Université de Montpellier, CNRS, Montpellier, France. [5]These authors contributed equally: Rudy Mevizou, Dana Naim, Serge Roche, Audrey Sirvent. ✉email: serge.roche@crbm.cnrs.fr; audrey.sirvent@crbm.cnrs.fr

Received: 7 March 2025 Revised: 17 November 2025 Accepted: 2 December 2025
Published online: 15 December 2025

the contribution of the mechanism to the oncogenic function of mTORC2, particularly in CRC, is poorly characterized.

The Src-Like-Adaptor Protein (SLAP) belongs to the family of small adaptor proteins and is a negative regulator of tyrosine kinase (TK) signaling receptors, particularly those activated by immune antigens and growth factors [18, 19]. Functionally, SLAP regulates the development and activation of thymocytes, where it is abundantly expressed [20, 21]. It also negatively regulates Receptor TK (RTK) signaling, leading to inhibition of fibroblast cell proliferation and migration [22–24]. Mechanistically, SLAP interacts with the E3 ligase CBL to induce receptor degradation [25–27]. SLAP shares high sequence homology with the N-terminus of TK SRC, including a myristoylation site and an SH3 and SH2 domain, hence its name [18]. Because of this homology, SLAP also inhibits SRC-like signaling, possibly by preventing SRC-RTK association and/or promoting degradation of SRC-like substrates via CBL, such as the LCK substrate ZAP70 during TCR signaling [22, 23, 28]. In a previous study, we reported that SLAP is also abundantly expressed in colonic epithelium and its expression level is significantly downregulated in CRC [29]. We also uncovered a tumor suppressor function of SLAP in CRC involving degradation of the RTK and SRC oncogenic substrate EPHA2. This activity did not require CBL but required interaction with the ubiquitination factor UBE4A, revealing the diversity of ubiquitination factors used by SLAP to mediate its inhibitory function [26]. Whether SLAP targets additional oncogenic signaling pathways to control CRC development remains to be determined.

In this study, we searched for additional SLAP signaling targets in CRC cells by proteomics. We show that mTORC2 is a major interactor of SLAP mediated by mLST8 binding. SLAP acts as an mTORC2 signaling inhibitor by promoting complex disassembly via non-degradative mLST8 ubiquitination and the novel SLAP interactor and E3 ubiquitin ligase UBE3C. Functionally, SLAP anti-oncogenic effect in CRC cells is mediated by mTORC2 inhibition. Collectively, our study identifies a novel dysregulation mechanism of mTORC2 complex integrity induced by SLAP downregulation with potential therapeutic utility in CRC.

MATERIALS AND METHODS

Antibodies: anti-SLAP (C-19) was from Santa Cruz; anti-EPHA2 (D4A2), anti-mTOR (7C10), anti-LST8 (#3227), anti-Raptor (24C12), anti-S6K1 (#9202), anti-pT389S6K1 (108D2), anti-AKT (#9272), anti-pS473AKT (D9AE), anti-Rictor (53A2 et D16H9), anti-NDRG1 (D8G9), anti-pT346 NDRG1 (D98G11), anti-ULK1 (8054S) and anti-pS555 ULK1 (14202T) were from Cell Signaling Technology; anti-Sin1 (D7G1A), anti-TRAF2 (4724), anti-Rictor (A300-459A and A300-458A) and anti-LST8 (A300-679A) were from Bethyl Labs; anti-Flag M2, anti-Flag M2 agarose and anti-Actin were from Sigma Aldrich; anti-Flag magnetic beads was from Termofisher (#A36797); anti-Telo2 (15975-1-AP) was from Protein Tech; anti-pan Ubiquitin was from Zymed; anti-Rictor (NBP1-51645SS) used for PLA was from NOVUS.

Drugs: mTOR inhibitors KU-0063794, Temsilorimus (TS), and AZD2014 were from Selleckchem (USA); PP242/Torkinib (#T2414) was from TargetMOL.

Vectors: pcDNA3 and retroviral pMX-pS-CESAR vectors expressing SLAP-Flag, SLAP SH3*(P73L)-Flag, SLAP SH2*(R111E)-Flag, and SLAP SH3*SH2*-Flag (a gift of A. Weiss, University of California, San Francisco, USA) and SLAP N32-Flag were described in [29]. pMXs-DsRed Express was a gift from Shinya Yamanaka (Addgene plasmid # 22724; www.addgene.org). Human RICTOR, RAPTOR, mTOR, SIN1, LST8, TTI1 and TEL2 cDNA was obtained from an ORFeome library (Montpellier genomic platform, GENOMIX, www.mgc.cnrs.fr) and subcloned into HA and Flag-tagged form in pcDNA3 and retroviral pMX-pS-CESAR expression vectors. Pol, GAG, and Env expression vectors were described in [29]. pRBG4 Ubiquitin-myc-6His WT K48R and K63R mutants were from J. Pierre (IGR, Université Paris-XI, France). pcDNA3-LST8 mutants and pRBG4 Ub-myc-6His K29R and K33R mutants were obtained using the QuickChange Site-Directed Mutagenesis Kit (Agilent) using the following oligonucleotides: mLST8 K86A: (F) CAGCTACGACGGCGTCAACAGGAACATCGCGTCTGTGGGC, (R) GCCCACAG ACGCGATGTTCCTGTTGACGCCGTCGTAGCTG; K215A: (F)CCCAGCTCATCC CCAAGACTAGGATCCCTGCCCACACGCGC, (R) GCGCGTGTGGGCAGGGATC CTAGTCTTGGGGATGAGCTGGG; K245A: (F)GCTCGGCTGATCAGACGTGCAG GATCTGGAGGACGTCCAACTTC, (R) GAAGTTGGACGTCCTCCAGATCCTGCA CGTCTGATCAGCCGAGC; K86R: CAGCTACGACGGCGTCAACAGGAACA TCGCGTCTGTGGGC (F), GCCCACAGACGCGATGTTCCTGTTGACGCCGTCGT AGCTG (R); K215R: CCCAGCTCATCCCCAAGACTAGGATCCCTGCCCACA CGCGC (F), GCGCGTGTGGGCAGGGATCCTAGTCTTGGGGATGAGCTGGG (R); Ub K29R: (F) CGAAAATGTGAAGGCCAGGATCCAGGATAAGGAAGGC, (R) GCCTTCCTTATCCTGGATCCTGGCCTTCACATTTTCG; Ub K33R: (F) GTGAAGG CCAAGATCCAGGATAGGGAAGGCATTCCCCCCGACC, (R) GGTCGGGGGGAA TGCCTTCCCTATCCTGGATCTTGGCCTTCAC.

siRNA: siSLA_h #1 (ON-TARGETplus Human SLA (6503) siRNA J-010815-07; Dharmacon), siSLA_h #2 (ON-TARGETplus Human SLA (6503) siRNA J-010815-08; Dharmacon), siLST8_h #1 (ON-TARGETplus Human MLST8 (64223) siRNA J-016093-05; Dharmacon), siLST8_h #2 (ON-TARGETplus Human MLST8 (64223) siRNA J-016093-06; Dharmacon), siLST8_h #3 (ON-TARGETplus Human MLST8 (64223) siRNA J-016093-07; Dharmacon), siLST8_h #4 (ON-TARGETplus Human MLST8 (64223) siRNA J-016093-08; Dharmacon), siLST8_h #5(UGACGGAGCUGAGCAUCAA), siRictor_h #1; ON-TARGETplus Human RICTOR (253260) siRNA J-016984-05, Dharmacon), siRictor_h #2 (ON-TARGETplus Human RICTOR (253260) siRNA J-016984-06, Dharmacon), siRaptor_h#1(ON-TARGETplus Human RPTOR (57521) siRNA J-004107-05, Dharmacon), siRaptor_ h #2 (ON-TARGETplus Human RPTOR (57521) siRNA J-004107-05; Dharmacon), siUBE3C_h #1 (GCCAGACAUUA-CUACUUCCUA), siTRAF2_h #1 (GGACCAAGACAAGAUUGAA), siTRIM32_h #1 (GAUCAGGGGUGGUCAAAUA).

shRNA vectors: control (CTRL, GACACTCGGTAGTCTATAC), shRICTOR (ACTTGTGAAGAATCGTATC) and shRAPTOR (GGCTAGTCTGTTTCGAAATTT) were subcloned into pSUPER.retro.neo.GFP. shSLAP (GACCTGGTGAACCAC-TATT) in pSiren-retroQ was described in [29].

Cell cultures, retroviral infections and transfections

HCT116, HT29, SW480, DLD1, LS174T, LoVo, SW620 and HEK293T cell lines were obtained from ATCC (Rockville, MD). DLD1 cells stably expressing TEL2-degron ($TEL2^{AID}$) (a gift of Dr D. Helmlinger, CRBM, Montpellier, France) were described in [30]. Cells were cultured at 37 °C and 5% CO_2 in a humidified incubator in Dulbecco's Modified Eagle's Medium (DMEM) GlutaMAX (Invitrogen) supplemented with 10% fetal calf serum (FCS), 100 U/ml of penicillin and 100 µg/ml of streptomycin as described in [29], and were routinely tested for Mycoplasma using MycoAlert Mycoplasma detection kit (Lonza, #LT07-318). Retroviral production and cell infection were performed as described in [29]. Stable cell lines were obtained by GFP and/or mRFP-fluorescence-activated cell sorting. Transient plasmid transfections in HEK293T cells were performed with the jetPEI reagent (Polyplus-transfection) according to the manufacturer's instructions. For siRNA transfection, 2.10^5 cells were seeded in 6-well plates and transfected with 20 nmol of siRNA and 9 µl of Lipofectamine RNAi Max according to the manufacturer's protocol (ThermoFisher Scientific).

Soft agar, invasion, colonospheres and tumoroid formation assays

Colony formation in soft-agar assays was performed from 1000 to 2000 cells per well that were seeded in 12-well plates in 1 ml DMEM containing 10% FCS and 0.33% agar (Sigma Aldrich)on a layer of 1 ml of the same medium containing 0.7% agar as described in [29, 31]. After 18–21 days, colonies with >50 cells were scored as positive. Cell invasion assay was performed in Fluoroblok invasion chambers (BD Bioscience) using 50,000 cells in the presence of 100 µl of 1–1.2 mg/ml Matrigel (BD Bioscience) as in [29, 31]. After 24–48 h, cells were labeled with Calcein AM (Sigma Aldrich) and invasive cells were photographed using the EVOS FL Cell Imaging System (ThermoFisher Scientific). Quantification of the number of invasive cells per well was done with the ImageJ software (https://imagej.nih.gov/ij/). For colonosphere formation, 100 cells were seeded in ultra-low attachment plates (Corning) in 100 µl of DMEM/F12 (Life Technologies) supplemented with 2mM L-glutamine, N-2 (Life Technologies), EGF (20 ng/ml, Bio-techne) and FGF (10 ng ml^{-1}—Bio-techne) for 7 days. Tumoroids formation was performed as follows: 3000 HCT116 cells were resuspended in advanced DMEM/F12 (Life Technologies) supplemented with 1% Penstrep, 2mM L-glutamine, N-2 (Life Technologies) and Matrigel (Corning) (1:2 ratio) prior to plating in 24-well plates. After polymerization of Matrigel, 0.5 mL DMEM/F12 supplemented with 20 ng/mL EGF and 10 ng/mL FGF (Biotechne) was added. Tumoroids were cultured at 37 °C and 5% CO2 in a humidified incubator and treated or not with the indicated drug (twice per week) for 7 days before size quantification by microscopy.

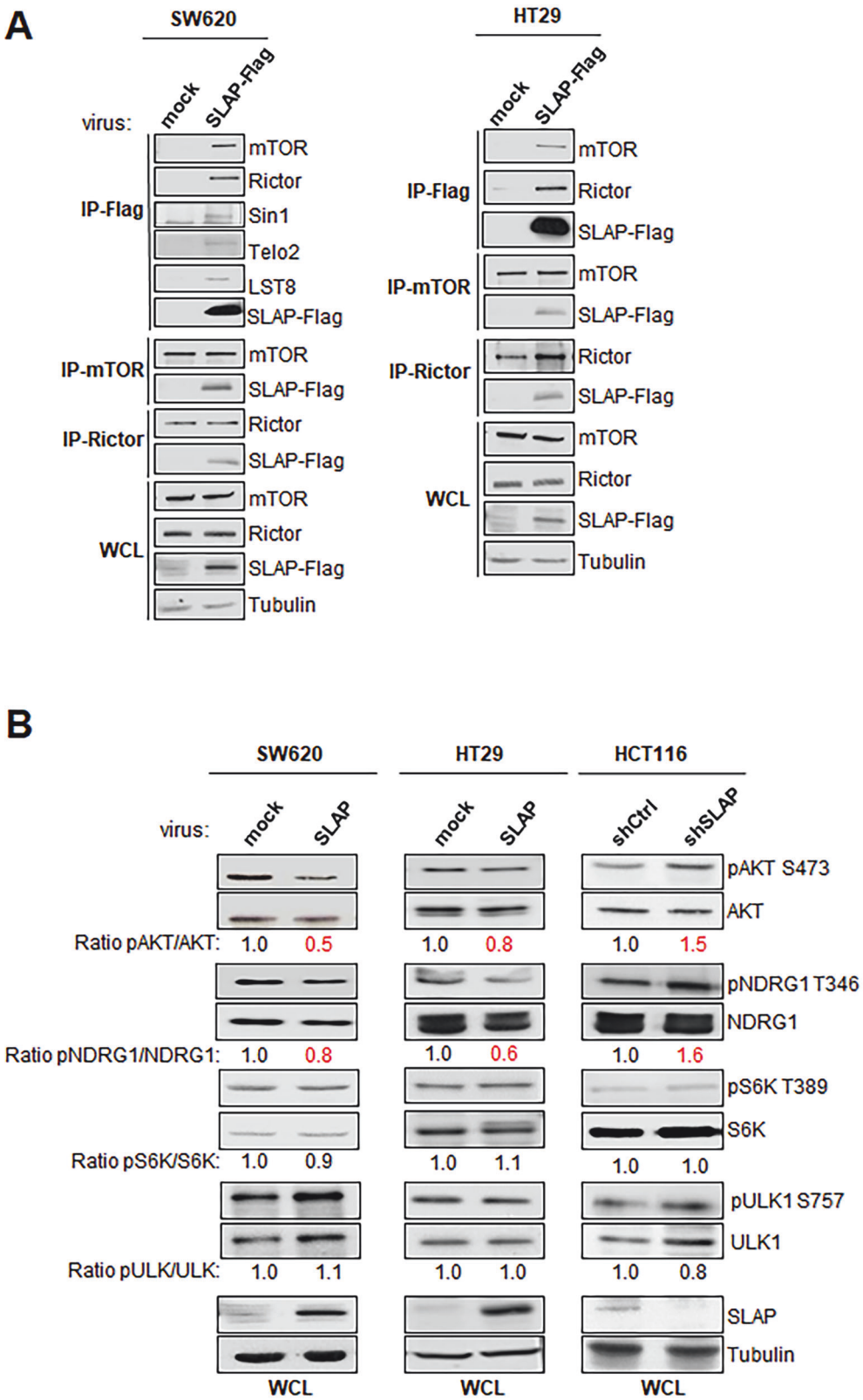

Fig. 1 SLAP Interacts with mTORC2. A Biochemical validation of SLAP-mTORC2 complex formation in indicated CRC cells. **B** Western blot (WB) analysis of SLAP-dependent phosphorylation of selected mTORC1/2 substrates in the indicated CRC cells. Shown are representative WB from three independent experiments.

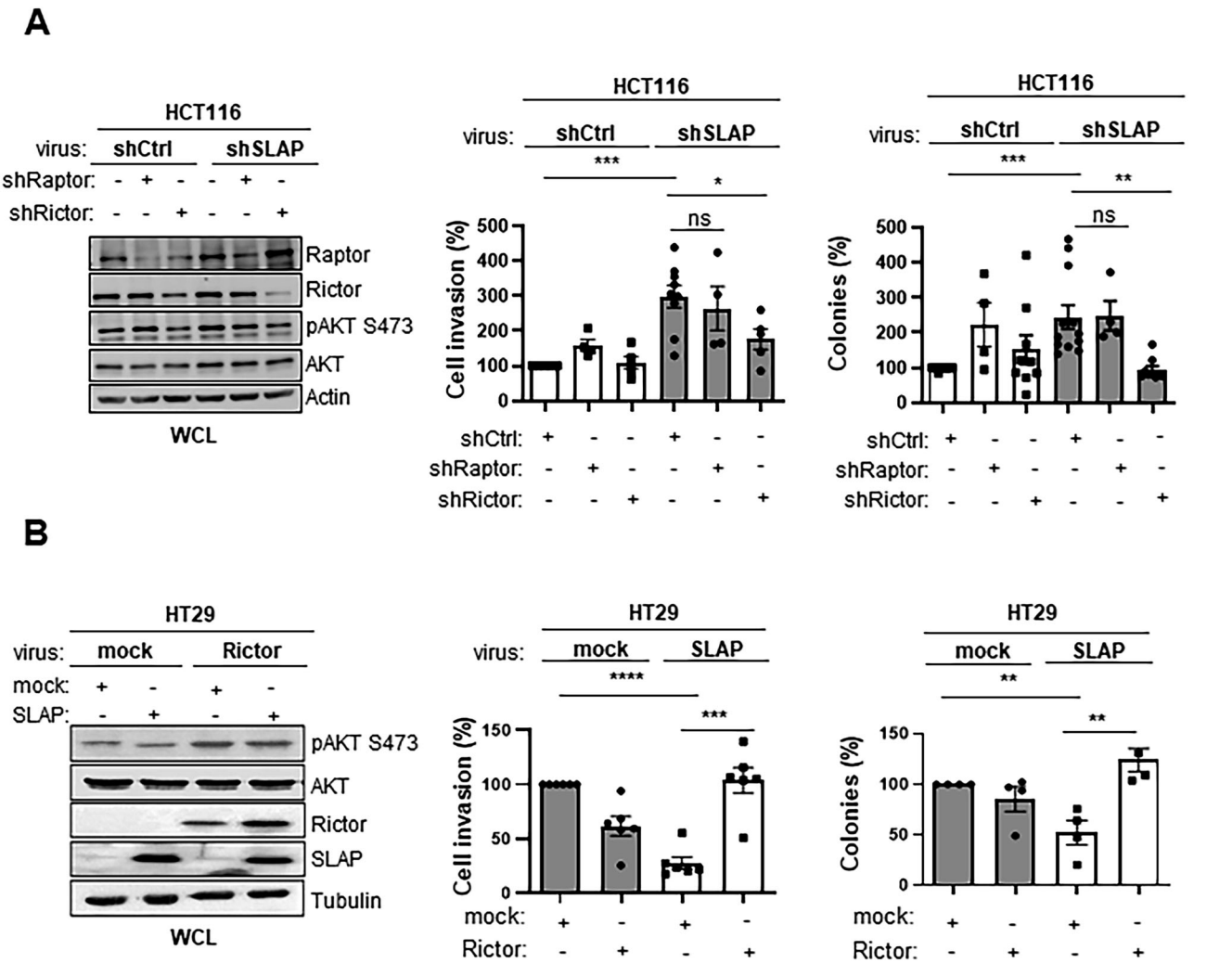

Fig. 2 SLAP anti-oncogenic function is mediated by mTORC2 inhibition. A HCT116 CRC cell transforming properties induced by SLAP depletion are dependent upon RICTOR but not RAPTOR expression. Left: WB of protein level in indicated HCT116 cells transduced with indicated retroviruses. Right: cell invasion in Matrigel (control: 100%) and colony formation in soft agar (number) is shown (mean ± SEM, $n = 3–5$). **B** SLAP-dependent inhibition of HT29 cell transforming properties is overcome by RICTOR overexpression. Left: WB of indicated protein levels in HT29 cells transduced with indicated retroviruses. Right: cell invasion in Matrigel colony formation in soft agar (control: 100%) is shown. Is shown the mean ± SEM, $n = 3–5$, $^{*}p \le 0.05$, $^{**}p \le 0.01$ (unpaired t-test).

RNA extraction and RT-quantitative PCR

mRNA was extracted from cell lines and tissue samples using the RNeasy Plus Mini Kit (Qiagen) according to the manufacturer's instructions. RNA (1 µg) was reverse transcribed with the SuperScript VILO cDNA Synthesis Kit (Invitrogen). Quantitative PCR (qPCR) was performed with the SyBR Green Master Mix in a LightCycler 480 (Roche). Expression levels were normalized with the Tubulin or GAPDH human housekeeping gene. Primers used for qPCR are: human TRIM32: (F) TGT GGT TTG GTG TTA TGT GAG C, (R) TAA GTT CCC GCA GAC GAG TTA; human TRAF2: (F) GCT CAT GCT GAC CGA ATG TC, (R) GCC GTC ACA AGT TAA GGG GAA; human UBE3C: (F) AAA GCA GAT AAG GTC ACT CAG C, (R) CAA AAG GCA ACT CTG TCA GGA.

Biochemistry

Immunoprecipitation (IP) and immunoblotting (WB) were performed as described in [29]. Briefly, cells were lysed at 4 °C with Triton-lysis buffer (20 mM Hepes pH7.5, 150 mM NaCl, 0.5% Triton X-100, 6 mM octyl β-D-glucopyranidose, 10 µg/ml aprotinin, 20 µM leupeptin, 1 mM NaF, 1 mM DTT and 100 µM Na3VO4) unless specified. For WB, antibodies were used at a dilution of 1:1000. For mTORC2 co-immunoprecipitation experiments, cells were lysed in CHAPS buffer [40 mM HEPES pH 7.5, 120 mM NaCl, 1 mM EDTA, 0.6% CHAPS 10 mM pyrophosphate, 10 mM glycerophosphate, 50 mM NaF, 1.5 mM Na3VO4, 1% Triton X-100, and EDTA-free protease inhibitors (Roche)] as described in [32]. Cycloheximide (50 µg/ml) cell treatment was performed as in [29]. For ubiquitination assays, cells were lysed at room temperature with Guanidine Buffer (6 M guanidinium-HCl, 0.1 M Na_2HPO_4/NaH_2PO_4, 0.01 M Tris/HCl, pH 8.0, 5 mM imidazole and 10 mM β-mercaptoethanol). Ubiquitinated proteins were purified using Ni-NTA agarose beads (Qiagen). Complexes were then washed in Guanidine buffer and then Urea buffer (8 M urea, 0.1 M Na_2HPO_4/NaH_2PO_4, 0.01 M Tris/HCl, pH 8.0, 10 mM β-mercaptoethanol, 0.1% Triton X-100) and analyzed by WB. GST pull-down assays were performed as described in [29]. The expression of fusion proteins in *Escherichia coli* (BL21 strain) was induced by incubation with 0.2 mM isopropyl β-D-thiogalactopyranoside at 25 °C for 3 h. The expressed proteins were purified as described in [29] and bound to Glutathione Sepharose 4B beads (GE Healthcare). 15 µg of GST alone, GST-SLAP N32 and GST-SLAP N3*2 bound to Glutathione Sepharose beads were incubated with transfected HEK293T cell lysates at 4 °C for 2 h. Complexes were washed in PBS and analyzed by WB. 20–50 µg of whole cell lysates were loaded on SDS-PAGE gels and transferred onto Immobilon membranes (Millipore). Detection was performed using the ECL System (Amersham Biosciences).

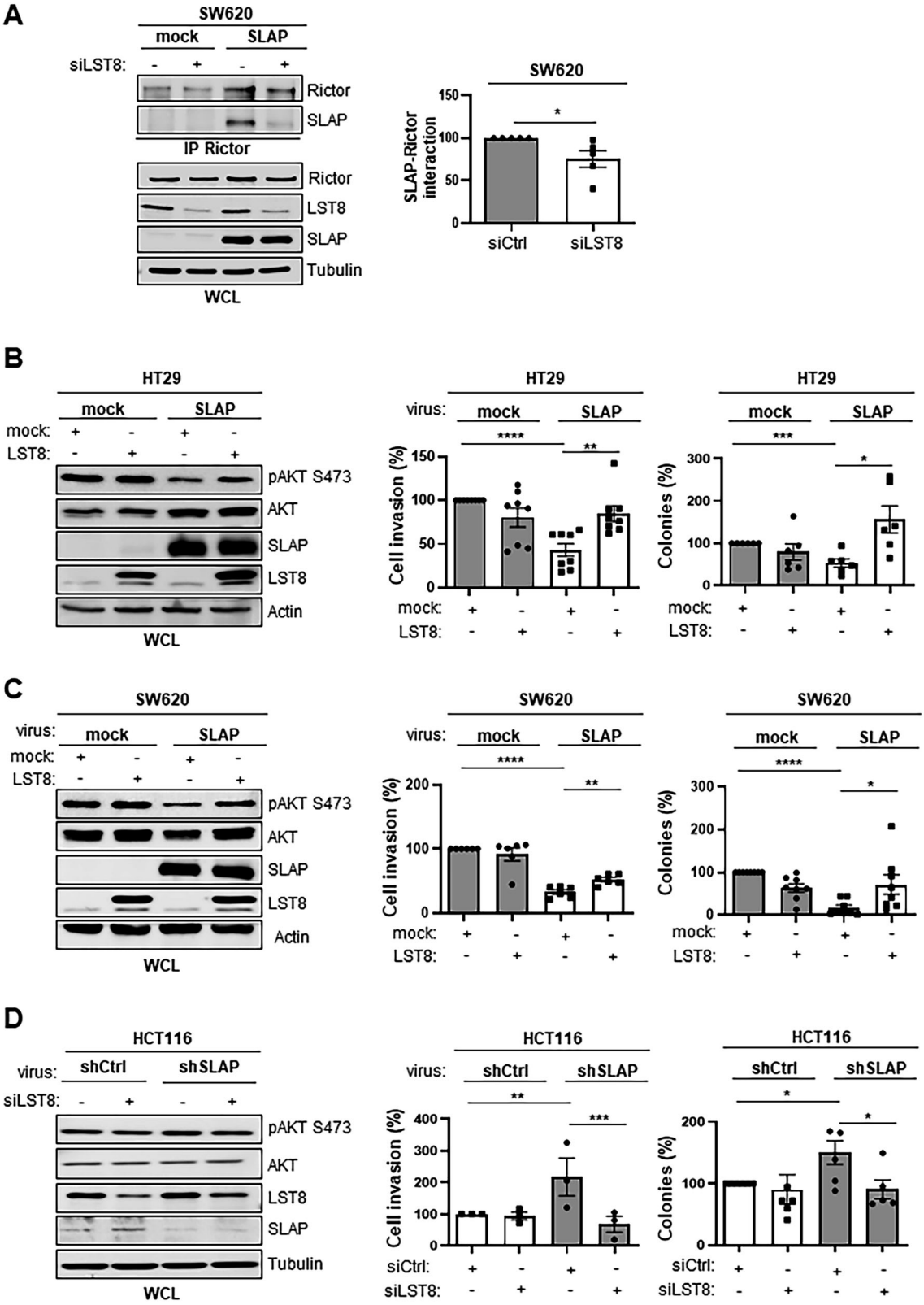

Proteomics

The Proteome Profiler Human Phospho-Kinase Array Kit was purchased from R&D Systems. CRC cells were lysed, and 300 µg of protein lysates were used for WB as described in [33]. Signals were quantified with the Amersham Imager 600 (GE Healthcare) from two independent biological replicates. SILAC-based interactomic analysis was performed as described in [29]. Briefly, SW620 cells were cultured in SILAC DMEM (Pierce) without Lysine (Lys) and Arginine (Arg) and supplemented with 4mM L-glutamine, 10% dialyzed FBS (Invitrogen), 0.084 g/l Arg and 0.146 g/l Lys. Heavy ($^{13}C_6{}^{15}N_4$-Arg and $^{13}C_6{}^{15}N_2$-Lys, from EurisoTop) or unlabeled amino acids

Fig. 3 SLAP associates with mLST8 to mediate its anti-oncogenic function. A SLAP-RICTOR interaction is mediated by mLST8 expression in SW620 cells. Left: co-immunoprecipitation of SLAP-FLAG with RICTOR in SW620 cells that were transfected with a control siRNA or a siRNA targeting LST8 (siLST8) as indicated. The level of SLAP, RICTOR and mLST8 is shown. Right: relative quantification of SLAP-RICTOR interaction (mean ± SEM, $n = 5$, $^*p \le 0.05$, unpaired t-test). SLAP inhibition of HT29 (**B**) and SW620 (**C**) cell transforming properties is overcome by mLST8 overexpression. Left: WB of indicated protein levels in HT29 cells transduced with indicated retroviruses. Right: cell invasion in Matrigel (control: 100%) and colony formation (number) in soft agar is shown. **D** Enhanced HCT116 cell transforming properties induced by SLAP depletion are mediated by mLST8 expression. Left: WB of protein level in indicated HCT116 cells transduced with indicated retroviruses and siRNA. Cell invasion in Matrigel and colony formation in soft agar (control: 100%) are shown as the mean ± SEM, $n = 3$–5, $^*p \le 0.05$, $^{**}p \le 0.01$, $^{***}p \le 0.001$ (unpaired t-test).

(light Arg and Lys, from Sigma Aldrich) were used. After 3 weeks of metabolic labeling, cells were lysed in CHAPS lysis buffer. Heavy and light lysates (30 mg of protein) were mixed and immunoprecipitated with anti-Flag M2 agarose overnight at 4 °C. Peptides obtained after digestion of IP were analyzed using a Qexactive-HFX system coupled with an RSLC-U3000 nano HPLC. Samples were desalted and pre-concentrated online on a Pepmap® precolumn (0.3 mm × 10 mm). A gradient consisting of 6–25% B for 100 min, 25–40% B for 20 min, 40–90% B for 2 min ($A = 0.1\%$ formic acid; $B = 0.1\%$ formic acid in 80% acetonitrile) at 300 nl/min was used to elute peptides from the capillary reverse-phase column (0.075 mm × 250 mm; Pepmap®, ThermoFisherScientific), fitted with a stainless steel emitter (Thermo Sientific). Spectra were acquired with the instrument operating in the data-dependent acquisition mode throughout the HPLC gradient. MS scans were acquired with a resolution set at 60,000. Up to twelve of the most intense ions per cycle were fragmented and analyzed using a resolution of 30,0000. Peptide fragmentation was performed using nitrogen gas on the most abundant and at least doubly charged ions detected in the initial MS scan and a dynamic exclusion time of 20 s. Analysis was performed with the MaxQuant software (version 2.0.3.0). All MS/MS spectra were searched using Andromeda against a decoy database consisting of a combination of the *Homo sapiens* reference proteome (release 2024_01 www.uniprot.org) and 250 classical contaminants, containing forward and reverse entities. A maximum of two missed cleavages was allowed. The search was performed with oxidation (M) and acetyl (protein N-term) as variable modifications, and carbamidomethyl (C) as a fixed modification. FDR was set at 0.05 for peptides and proteins, and the minimum peptide length was 7.

PLA and cell imaging

Proximity ligation assay (PLA) was performed according to the manufacturing kit protocol (#NF.100.2, Navinci). Briefly, SW620 cells plated on glass coverslips for 48 h were fixed with 4% paraformaldehyde, 0.5% triton during 20 min at room temperature. Glass slides were blocked in the Navinci® Blocking Buffer (1x) during 1 h at 37 °C in a humidity chamber and then incubated with primary antibodies anti-RICTOR (NOVUS NBP1-51645SS, 1:400, mouse) and anti-mTOR (CST#2983, 1:400 rabbit) in the Navinci® Primary Antibody Diluent (1X) overnight at 4 °C. After the washing steps, glass coverslips were incubated 1 h at 37 °C in a humidity chamber with the Navenibodies diluted (1:40 each) in Navenibody Diluent. After three washes, three enzymatic reactions followed. The enzyme (A,B,C) was diluted (1:40) in the associated buffer (A,B,C) (1:5) and glass coverslips were incubated respectively 60 min, 30 min and 90 min at 37 °C in a humidity chamber. Finally, after washes glass coverslips were mounted with the Duolink® In Situ Mounting Medium with DAPI (#DUO82040) and observed with an upright fluorescent microscope. Images were acquired using Zeiss Axioimager Z2 microscope (20–80 cells/field, 7–15 fields per coverslip), with objective plan-apochromat 63x/1.40 oil, then PLA signal area analysis was processed using Fiji software (https://fiji.sc/).

Animal experiments

In vivo experiments were performed in compliance with the French guidelines for experimental animal studies (Direction des services vétérinaires, ministère de l'agriculture, France, APAFIS #35916-2022031511382008 v6, local animal house agreement number F3417216). 2×10^6 SW620 cells (or derivatives) were subcutaneously injected in the flank of 5-week-old female athymic nude mice (Envigo). Tumor volumes were measured at the indicated intervals using calipers for 24 days. For drug treatment, HCT116 cells (or derivative) were first cultured for 2 weeks in suspension to form colonospheres in low attachment T150 flasks (Sigma); 150,000 dissociated cells (using Accumax solution, Invitrogen) mixed with Matrigel (Corning, ratio 1:1) were injected into 7-old female athymic nude mice (Charles River Laboratories, France). When tumor volume reached 50 mm^3, mice were randomized and treated with vehicle (0.5% methylcellulose/0.05% Tween80) or Torkinib (PP242; 40 mg/kg) by oral gavage daily, 5 days/week for 21 days. Animals were excluded upon reaching ≥20% weight loss, evidence of tumor necrosis, or the presence of multilobulated tumors. Tumor xenografts were excised, weighed and cryopreserved or processed for subsequent immunohistochemical (IHC) or protein tissue analysis by WB as described in [29, 31]. In vivo siRNA administration in $APC^{\Delta 14/+}$ mice was described in [29]. Briefly, murine Slap AGAUUGGUAGCUUCAUGAU or control CGUACGCGGAAUACUUCGATT siRNAs (10 µg) were mixed and complexed at room temperature for 30 min with an equal volume of cationic liposomes (60 nmol, generous gift from V. Escriou, Paris Descartes University, France) [29] in 0.9% NaCl incubated. Then, 3 week/old $APC^{\Delta 14/+}$ mice (a gift of C Perret, Cochin Institute, Paris) received i.p. injections of siRNA twice a week for 6 weeks. Five days after the last injection, intestinal tumors were counted, measured, removed and cryopreserved. A double-blind protocol was used. Blinding was not applied to the subcutaneous tumor growth, but at least two independent experimenters performed cell culture, injections, treatments, and measurements. Group labels were assigned to cages, but expected outcomes were unknown to the experimenters during data collection, minimizing bias.

Immunohistochemical analysis

For bright field immunochemistry, sections were treated with BIOXALL (Vector Laboratories) for 10 min before blocking and incubation with primary antibodies (anti-pSer473 AKT, D9AE 1:50 according to CST protocol). Secondary staining was detected with DAB (Vector Laboratories), and sections were counterstained with hematoxylin (Sigma-Aldrich) and mounted with mounting medium (Pertex). For histological examination, tissue sections were deparaffinized and stained with hematoxylin, eosin, and alcian blue.

Statistical analysis

All analysis were performed using GraphPad Prism (9.3.1). Data are presented as the mean ± SEM from at least three independent experiments as stated. When distribution was normal (assessed with a Shapiro–Wilk test), the two-tailed t-test was used for between-group comparisons. In the other cases, the Mann–Whitney test was used. Statistics were carried out on a minimum of three independent experiments. The statistical significance level is illustrated with p values: $^*p \le 0.05$, $^{**}p \le 0.01$, $^{***}p \le 0.001$.

RESULTS

SLAP interacts with mTORC2

To identify novel SLAP targets in CRC cells, we performed SILAC-based interatomic analysis of SW620 CRC cells, which express low *SLA* mRNA level (i.e., SLAP-low) [29], by overexpressing a SLAP-Flag construct (Fig. S1A). A total of 164 proteins with a log ratio >1.5 were retrieved in ≥2/3 independent experiments with ≥3 peptides (Fig. S1B and Table S1). Gene Ontology analysis of SLAP interactors revealed strong enrichment in the mTOR pathway, followed by vesicular trafficking and mitochondrial functions (Fig. S1C). Consistent with this, we identified mTORC2 components—including mTOR, RICTOR, SIN1/MAPKAP1 (SIN1), and mLST8—demonstrating that mTORC2 is a novel SLAP target in CRC cells (Fig. S1 and Table S1). The PIKKs co-chaperones TELO2 and TTI1 were also identified, suggesting that SLAP may also bind to mTORC2 during

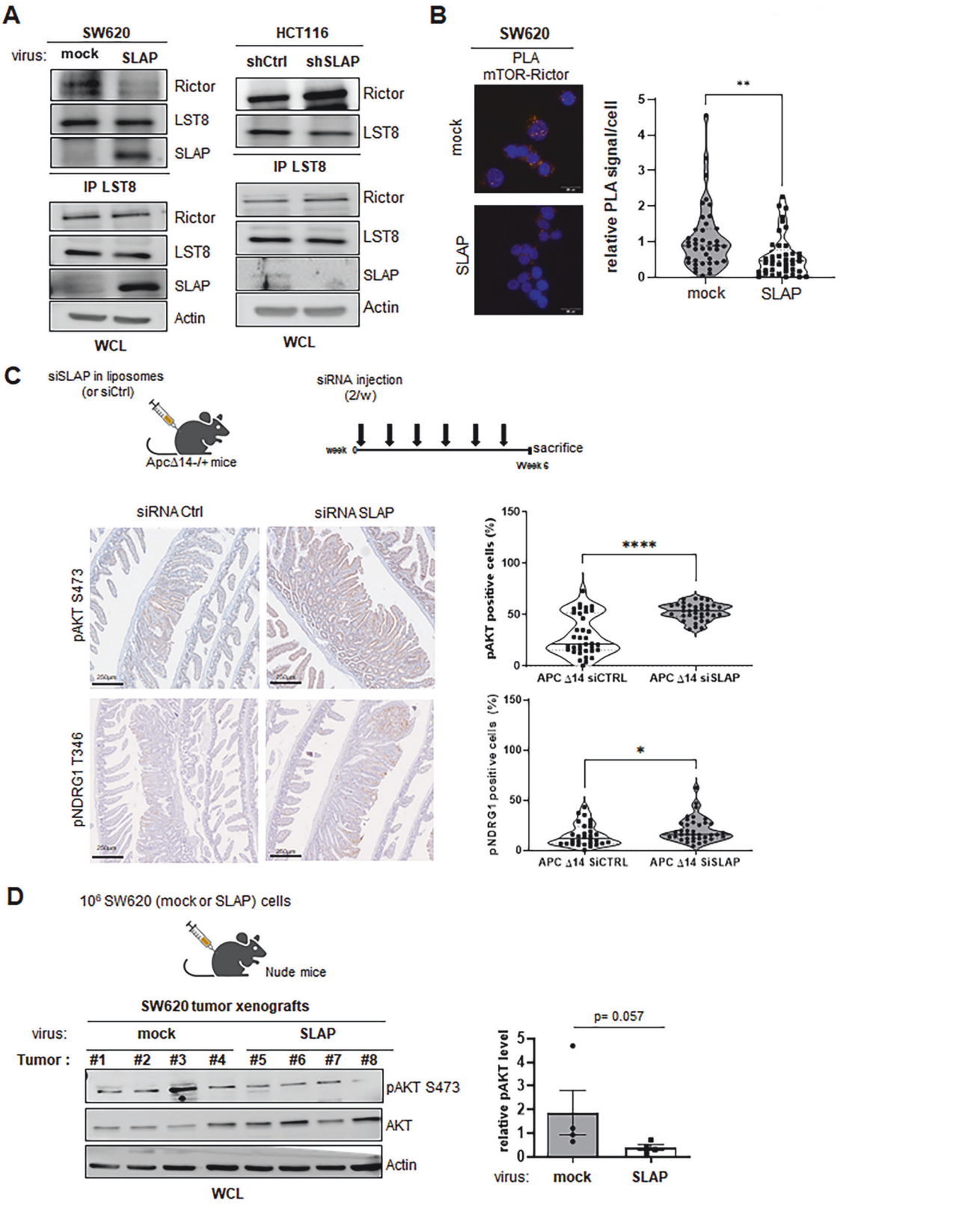

complex formation (Fig. S1 and Table S1). SLAP interaction with all mTORC2 components was next confirmed biochemically from cell lysates of SLAP-low HT29 and SW620 cells [29] by overexpressing SLAP-Flag (Fig. 1A). The effect of SLAP on mTORC2 phospho-signaling in CRC cells was next assessed with a phospho-kinase array (Fig. S2A). The phosphorylation level of specific mTORC2 substrates (pS473 AKT, pS9 GK3β), but not of mTORC1 (pT398 S6K and pT412/S424 S6K), was reduced upon SLAP expression, whereas their levels were increased upon shRNA-mediated SLAP silencing in HCT116 CRC cells, which retain a

Fig. 4 SLAP controls mTORC2 activity by regulating complex integrity. A mLST8-RICTOR interaction, necessary for mTORC2 activity, is controlled by SLAP expression in CRC cells. Association of mLST8 with RICTOR as assessed by co-immunoprecipitation from indicated CRC cells that were transduced with the indicated retrovirus. The level of SLAP, RICTOR and mLST8 is shown. The level of pS473 AKT is also assessed as a readout of mTORC2 activity. **B** The effect of SLAP expression on mTORC2 assembly in SW620 cells. A representative example (left) and its quantification (right) of endogenous mTOR-RICTOR interaction in SW620 cells expressing or not SLAP by PLA. Is shown a violin representation of deduced average PLA signal (20–80 cells per field, 7–15 fields analyzed/replicate, $n = 4$); $^{**}p < 0.01$ (Mann-Whitney test). **C** SLAP silencing increases mTORC2 activity in murine intestinal adenoma. Top: schematic of siRNA-mediated Slap silencing in ApcΔ14 ± mice. Bottom: a representative example (left) and quantification (right) of pS473 Akt and pT346 NDRG1 positive cells in intestinal adenoma of mice treated with indicated siRNA. Is shown the mean ± SEM of 5–7 area/mice, $n = 5$ mice per group; $^{*}p < 0.05$, $^{***}p < 0.001$ Mann-Whitney test. **D** SLAP controls mTORC2 activity in SW620 tumor xenografts in nude mice. Top: schematic of CRC tumor xenograft development; (bottom): WB analysis (left) and the quantification (right) of pS473 AKT levels (pAKT/AKT level) in indicated tumors (mean ± SEM, $n = 4$, Mann-Whitney test, p is indicated).

substantial level of endogenous SLAP (i.e., SLAP-high) [29]. This mTORC2 signaling inhibition by SLAP was confirmed by western blotting on specific substrates, including AKT and NDRG1, while the phosphorylation levels of the mTORC1-specific substrates S6K and ULK1 were unchanged [1] (Figs. 1B and S2B). Consistent with this, mTORC2-AKT signaling induced by growth factor stimulation in SW620 and HCT116 cell lines was modulated by SLAP expression, in contrast to mTORC1-S6K phospho-signaling (Fig. S2C, D). Thus, we concluded that SLAP specifically inhibits mTORC2 activity in CRC cells.

mTORC2 inhibition mediates SLAP anti-oncogenic function

We next investigated the contribution of mTORC2 signaling to the anti-oncogenic function of SLAP in CRC cells. SLAP depletion in HCT116 cells leads to an increase in anchorage-independent growth in soft agar and cell invasion in Matrigel [29] (Fig. 2A). This transformation-promoting effect was reversed by mTORC2 inhibition mediated by shRNA-mediated RICTOR knockdown. In contrast, mTORC2 inhibition had no significant effect in control cells, demonstrating the SLAP-dependent transforming effect. In addition, mTORC1 inhibition induced by shRNA-mediated RAPTOR depletion has no clear effect (Fig. 2A), confirming the mTORC2-dependent SLAP effect. Conversely, the inhibition of these transforming properties in HT29 cells by SLAP overexpression was overcome by RICTOR overexpression (Fig. 2B). RICTOR also restored mTORC2 activity, as shown by pS473 AKT (Fig. 2B) and mTORC2 complex formation (Fig. S3A), consistent with an mTORC2-dependent rescue effect of RICTOR. Finally, anchorage-independent cell growth and invasive properties of the metastatic CRC cell line SW620 were inhibited by RICTOR, but not by RAPTOR depletion, revealing a specific mTORC2 oncogenic function in these cells (Fig. S3B, C). However, this mTORC2 function was not evident upon SLAP overexpression (Fig. S3B, C), confirming that the mTORC2 oncogenic function can be inhibited by SLAP expression in CRC cells.

SLAP targets mLST8 to inhibit mTORC2 complex stability

To address the mechanism by which SLAP inhibits mTORC2 activity, we first examined the interaction between SLAP and each component of the complex, which was expressed in HEK293T cells. TELO2 and mLST8 were identified as the major SLAP interactors (Fig. S4A). Structure-interaction analysis of SLAP mutants harboring inactive mutations in the SH2 and/or SH3 domains (SH2*, SH3*, SH3*SH2*) or a deletion of the C-terminal domain (N32) revealed a contribution of SLAP-SH3 and -SH2 in the association with the mTORC2 complex in SW620 cells (Fig. S4B). In vitro pull-down assays, using purified GST-SLAP N32 with lysates from HEK293T cells expressing TELO2 or mLST8, confirmed specific interactions with these mTORC2 components. Notably, the interaction with mLST8 was reduced when using GST-SLAP SH3*, but not with TELO2, implicating a SH3-dependent binding to mLST8 (Fig. S4C). However, the functional interdependence of SH2 and SH3 domains in SLAP proteins, due close association through β-sheet formation [34] does not rule out any contribution of its SH2 in LST8 interaction. Similarly, the partial inhibition observed with GST-SLAP N32* (Fig. S4C) suggests an additional SH2/SH3-independent interaction with mLST8. Having established a role for SLAP SH2/SH3 domains in mTORC2 association in CRC cells, we hypothesized that mLST8 is involved in this molecular process. Consistent with this, siRNA-mediated depletion of mLST8 reduced SLAP association with RICTOR in both SW620 and HT29 cells (Figs. 3A and S4D). Functionally, mLST8 overexpression in HT29 and SW620 cells partially restored cell growth and invasion, which had been inhibited by SLAP expression (Fig. 3B, C), while siRNA-mediated mLT8 depletion reversed the transformed character of HCT116 cells that has been increased upon SLAP silencing. The depletion of mLST8 also reduced mTORC2 activity, as shown by pS473 AKT levels, consistent with an mTORC2-dependent effect of mLST8 depletion on these cellular responses (Fig. 3D). In contrast, TELO2 depletion did not reduce SLAP-RICTOR association in CRC cells (Fig. S5A), indicating that it is not involved in SLAP-mTORC2 complex formation. Furthermore, TELO2 overexpression in HT29 cells did not affect the SLAP-inhibitory effect on cell growth and invasion (Fig. S5B, C). Thus, we conclude that mLST8, but not TELO2, plays an important role in this SLAP-mTORC2 signaling process.

Since SLAP acts by promoting the degradation of signaling proteins, we evaluated the effect of SLAP on mLST8 protein stability. However, we did not observe any significant effect of SLAP on mLST8 levels, nor on additional mTORC2 components (Fig. S6A). Inhibition of protein synthesis by cycloheximide treatment of SW620 cells did not show any SLAP effect on mLST8 protein turnover (Fig. S6B). Thus, these data do not support a degradation mechanism involved in the regulation of mTORC2 by SLAP. We next examined the effect of SLAP on the integrity of the mTORC2 complex, which is required for activity. Although mLST8 is a common component of mTORC1 and 2, mLST8 is not required for mTORC1 activity, whereas it plays a key role in mTORC2 assembly [3]. Co-immunoprecipitation assays revealed that SLAP expression decreased mLST8 association with RICTOR in SW620 cells, whereas SLAP depletion in HCT116 cells increased this interaction (Fig. 4A). Similar results were obtained for mTOR-RICTOR association (a readout of mTORC2 assembly) in SW620 cells by PLA, in which protein pairs separated by a distance of less than approximately 40 nm were detected using fluorescent probes (Fig. 4B).

We next investigated the effect of SLAP expression on mTORC2 signaling in vivo, by focusing on pS473 AKT level as a readout of mTORC2 activity in experimental CRC models. In $Apc^{\Delta 14/+}$ transgenic mice, which develop Wnt pathway-driven intestinal tumors, we previously reported that siRNA-mediated inhibition of *Slap* expression in vivo increased the number and size of tumors [29]. Interestingly, IHC analysis revealed elevated pS473 AKT levels in intestinal adenoma of mice treated with siRNA against Slap (Fig. 4C, top panels). Similar results were observed on pT346 NDRG1, which was used additional readout of mTORC2 activity in these tumors (Fig. 4C, bottom panels). Finally, in human CRC xenografts in nude mice, we reported that SLAP overexpression

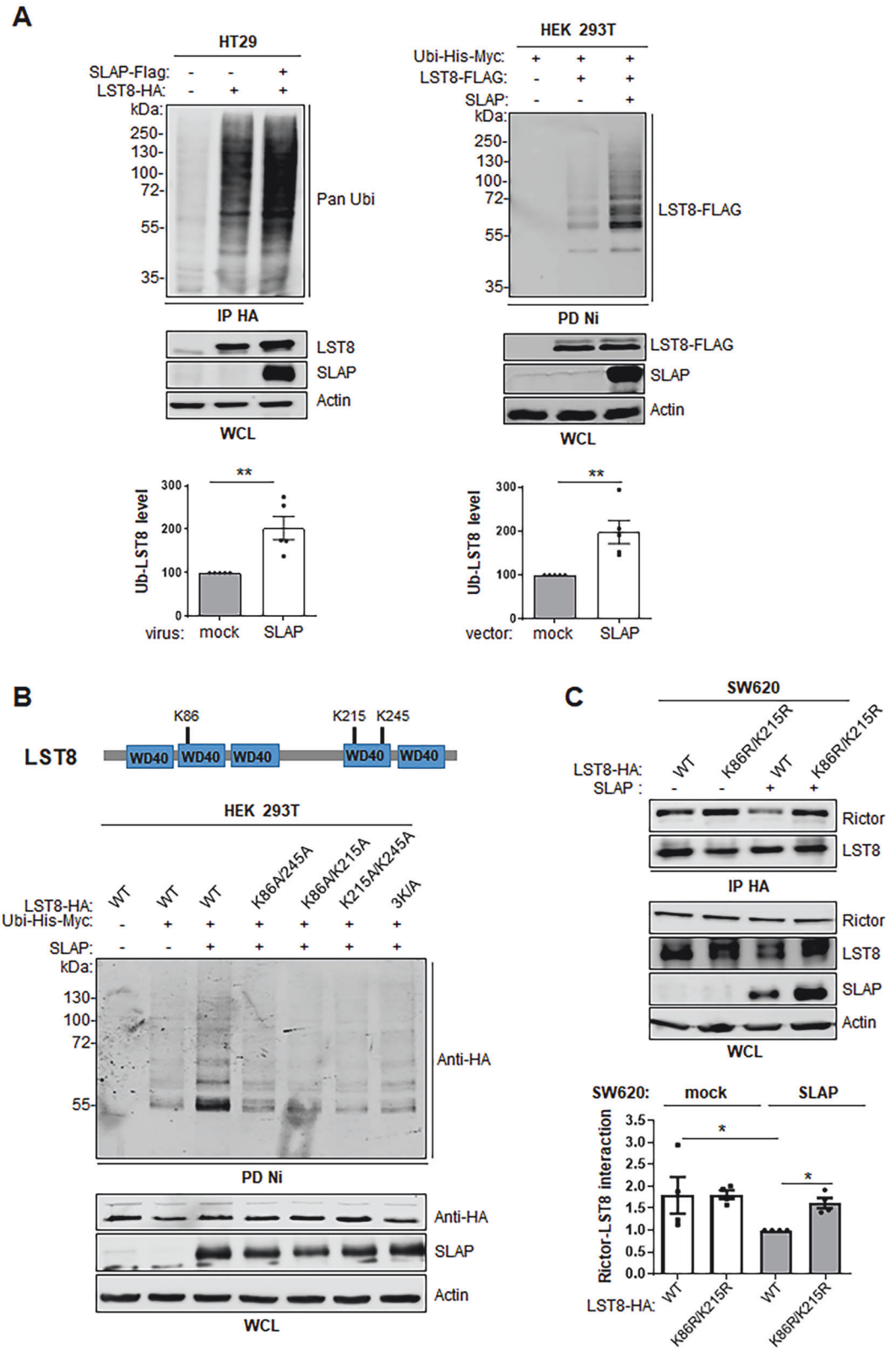

Fig. 5 SLAP regulates mTORC2 assembly via LST8 ubiquitination. A SLAP expression increases HA-LST8 ubiquitination in HEK293T and HT29 cells. WB analysis (top) and the quantification (bottom) of HA-mLST8 ubiquitination from cells overexpressing or not SLAP, as shown. Is shown the mean ± SEM, $n = 3–5$, $^{**}p \leq 0.01$, (unpaired t-test). **B** Mutagenesis analysis of SLAP-dependent HA-mLST8 ubiquitination in HEK293T cells. Is shown the schematic (top) and the mutagenesis analysis (bottom) of SLAP-dependent mLST8 ubiquitination sites as assessed by WB analysis (representative example of 3 independent experiments). **C** A mLST8 mutant resistant to SLAP-induced ubiquitination (LST8 K86R/K215R) reverses the inhibitory effect of SLAP on mTORC2 complex formation in CRC cells. Top: association of indicated mLST8-HA proteins with RICTOR as assessed by co-immunoprecipitation from HT29 cells that were transduced with indicated retrovirus. The level of SLAP, RICTOR and mLST8 is shown. Bottom: relative quantification of LST8-RICTOR association (mean ± SEM, $n = 3$, $^{**}p \leq 0.01$, Mann-Whitney test).

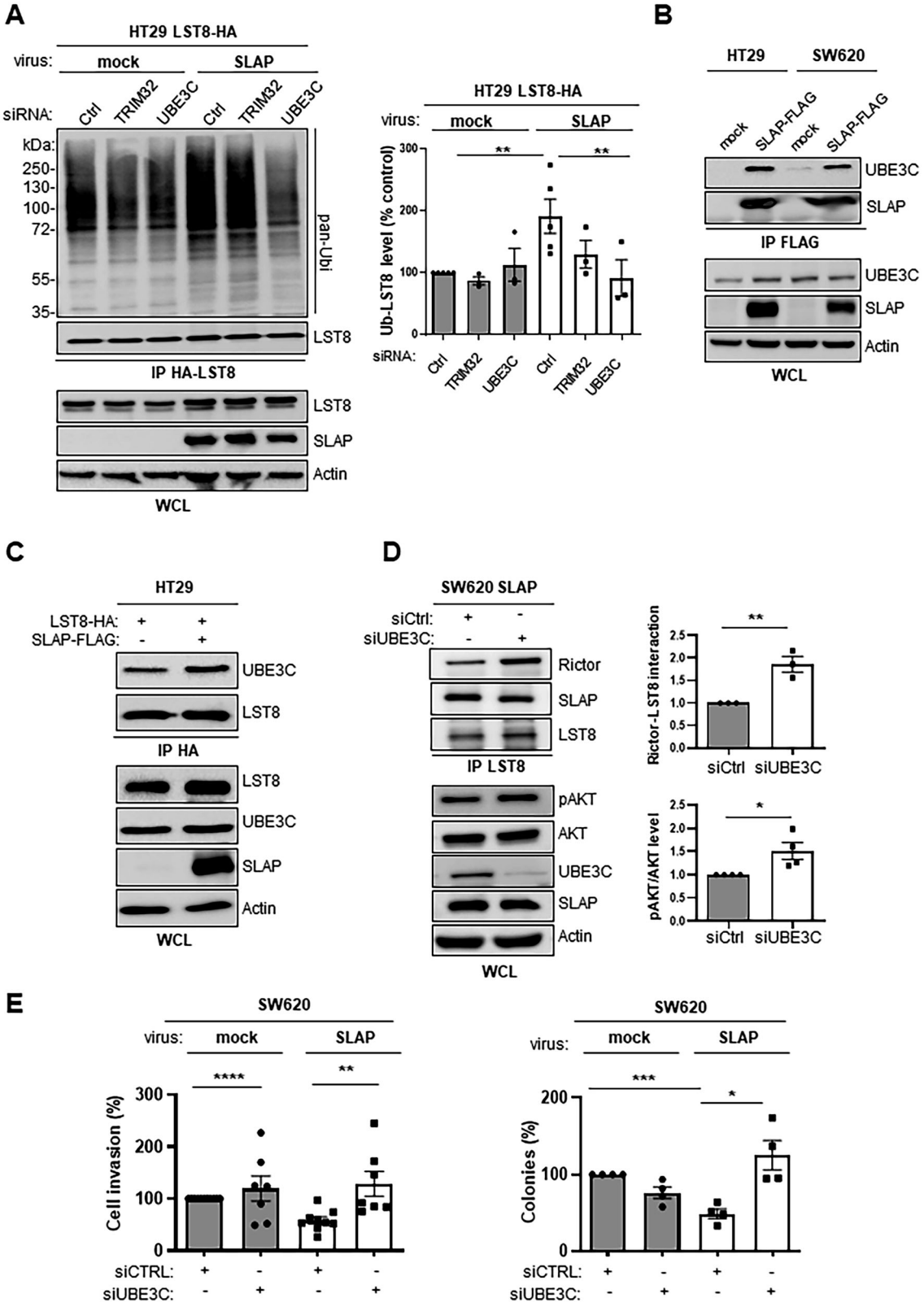

reduces tumor development in SW620 CRC tumors [29]. Western blotting analysis from these tumor lysates revealed a reduction of pS473 AKT tumor levels by SLAP overexpression (Fig. 4D). Taken together, these data indicate that SLAP inhibits mTORC2 activity by promoting complex disassembly via its interaction with mLST8.

A SLAP-UBE3C complex induces mLST8 ubiquitination and mTORC2 disassembly

To address the underlying mechanism of mTORC2 disassembly, we turned to an mLST8 ubiquitination mechanism activated by SLAP. mLST8 expression in HT29 cells already displays a high level

Fig. 6 SLAP interacts with UBE3C to facilitate LST8 ubiquitination and mTORC2 inhibition. A SLAP-dependent HA-mLST8 ubiquitination in HT29 cells is dependent upon UBE3C expression. Is shown the ubiquitination level of purified HA-mLST8 from lysates of HT29 cells expressing SLAP or not (control) and transfected with indicated siRNA targeting SLAP- associated ubiquitination factors. Left: a representative example; right: quantification (control: 100%); mean ± SEM, $n = 3–5$, $^{**}p \leq 0.01$ (Mann-Whitney test). **B** SLAP association with UBE3C in HT29 and SW620 CRC cells. **C** SLAP expression enhances HA-mLST8-UBE3C association in HT29 cells. **D** UBE3C depletion enhances mLST8-RICTOR association in SLAP overexpressing SW620 cells. left: association of mLST8 with RICTOR assessed by co-immunoprecipitation from SW620-SLAP cells (top) and WB of the level of SLAP, UBE3C, AKT and pS473 AKT, as a readout of mTORC2 activity (bottom). right: WB quantification; mean ± SEM, $n = 3–4$, $^{**}p \leq 0.01$ (unpaired t-test). **E** SLAP inhibition of SW620 cell transforming properties is overcome by UBE3C depletion. Colony formation in soft agar and cell invasion in Matrigel (control: 100%) are shown. Are shown the mean ± SEM, $n = 3–5$, $^{*}p \leq 0.05$, $^{**}p \leq 0.01$, $^{***}p \leq 0.001$ (unpaired t-test).

of ubiquitination, while SLAP expression further induced a two-fold increase (Fig. 5A, left panel). Similar results were obtained in HEK293T cells (Fig. 5A, right panel). We took advantage of this cell system to dissect the ubiquitination process activated by SLAP. First, we found that K/R mutation of Ubiquitin (Ubi-His-Myc) on K29 and K33 reduced the SLAP-mediated Ubiquitination effect on mLST8, in contrast to K48 and K63 mutations (Fig. S7). This data indicates that SLAP preferentially induces mLST8 ubiquitination branching on K29 and K33, consistent with a non-degradative mechanism of LST8 ubiquitination (Fig. S7). By mutagenesis analysis (K to A substitution) of mLST8 ubiquitination sites identified from the proteomic database PhosphoSitePlus, we found that SLAP-induced mLST8 ubiquitination occurs at K86, K215, and K245. Both the single-point mutants and the triple mutant (mLST8 K86A/K215A/K245A, i.e., 3 K/A) displayed markedly reduced ubiquitination in this assay (Fig. 5B). We then evaluated the contribution of these ubiquitination sites to SLAP-dependent mTORC2 complex disassembly. In SLAP-low HT29 cells, expression of the mLST8 K86R/K215R mutant did not affect mTORC2 complex formation (Fig. 5C). However, in cells overexpressing SLAP, co-immunoprecipitation assays revealed that, unlike the wild-type mLST8 (WT), this mutant restored mTORC2 assembly (Fig. 5C). Together, these findings support the model that SLAP inhibits mTORC2 activity by promoting complex disassembly through interaction with mLST8, and suggest that suggest that non-degradative ubiquitination of mLST8 at K86 and K215 is critical for this regulatory mechanism.

Next, we searched for ubiquitination factors involved in this SLAP signaling mechanism. Since TRAF2 was originally reported to be involved in mTORC2 disassembly [16], we tested whether this ubiquitination factor was involved in this SLAP effect. However, in contrast to mLST8, we did not detect any association between TRAF2 and SLAP in SW620 and HT29 cells (Fig. S8A), consistent with our proteomic analysis, which also failed to detect TRAF2 as a SLAP interactor (Table S1). Functionally, we did not observe a clear rescue effect of siRNA-mediated TRAF2 depletion on SLAP-induced SW620 cell invasion (Fig. S8B, C). These data are inconsistent with a major role for TRAF2 in SLAP signaling in CRC cells. In addition to mTORC2, our interactomic analysis uncovered several novel ubiquitination factors as SLAP interactors in SW620 cells (Fig. S1 and Table S1), including LTN1, UBE3C, UBR5, TRIM25 and possibly TRIM32 (retrieved in 1/3 experiments). We focused on UBE3C because of its reported capacity to induce K29 and K33 ubiquitination branches [35–37]. We found that siRNA-mediated depletion of UBE3C specifically reversed SLAP-induced mLST8 ubiquitination in HT29 cells, while it had no significant inhibitory effect at the basal level (Fig. 6A). In contrast, depletion of TRIM32, which reportedly induce K48 and K63 ubiquitination [38, 39], had no such inhibitory effect on this SLAP response (Fig. 6A). Thus, these data implicate UBE3C as an E3 ligase involved in this SLAP ubiquitination process on mLST8. Furthermore, UBE3C was associated with SLAP in HT29 and SW620 cells (Fig. 6B). SLAP expression also increased the association between UBE3C and mLST8 in HT29 cells (Fig. 6C). Consequently, UBE3C silencing enhanced mTORC2 assembly, which was inhibited by SLAP expression, as shown by mLST8-RICTOR association, and activity, as shown by pS473 AKT level, in SW620 cells (Fig. 6D). Functionally, siRNA-mediated UBE3C depletion specifically rescued the SW620 cell invasion and anchorage-independent cell growth, which had been inhibited by SLAP (Fig. 6E and S9A). In contrast, TRIM32 silencing has no such effect, demonstrating UBE3C specificity (Fig. S9A, B). Collectively, these data reveal a SLAP-UBE3C ubiquitination mechanism in the control of mTORC2 assembly in CRC cells.

SLAP influences CRC cell response to mTOR inhibitors

Having shown that SLAP defines a novel control mechanism of mTORC2 oncogenic function in CRC cells, we investigated whether it also influences CRC cell response to mTORC2 inhibitors. Since there are no specific mTORC2 inhibitors in clinical development, we used the mTOR catalytic inhibitor (mTORCi) KU-0063794, which targets both mTORC1 and mTORC2 [40, 41]. We also examined the effect of the mTORC1-specific inhibitor Temsilorimus (TS) [42] to evaluate the contribution of mTORC1 activity in this response. We found that anchorage-independent cell growth and cell invasion of HT29 cells was strongly inhibited by KU-0063794 treatment (100 nM) in contrast to TS (1 μM), indicating the mTORC2-dependent inhibitory effect (Fig. 7A). This mTORCi inhibitory response was not evident upon expression of SLAP, which already inhibits mTORC2 activity (Fig. 7A). Note that TS had a paradoxical promoting effect on pS473 AKT level in SLAP-expressing cells (Fig. 7A, top panel), which was attributed to a robust increase in mTORC2 activity, likely due to feedback mechanisms between mTORC1 and mTORC2 activity [40, 43]. Similar results were observed in SW620 cells, further validating our findings (Fig. S10A, B). Conversely, KU-0063794 strongly inhibited the transforming effects induced by SLAP depletion in HCT116 cells, while TS had no effect, which confirms the mTORC2-dependent response (Fig. 7B). In contrast, KU-0063794 had no inhibitory effect in control cells (i.e., shCTRL HCT116 cells), likely due to substantial SLAP-dependent mTORC2 inhibition in these cells (Fig. 7B). In fact, these mTOR inhibitors resulted in a paradoxical promoting effects, as exemplified on anchorage-independent cell growth (Fig. 7B), and for TS on pS473 AKT levels (Fig. 7B), possibly due to feedback mechanisms between mTORC1 and mTORC2 activity [40]. Consistent with these data, we observed a good correlation between SLAP expression, pS473 AKT levels, and the anti-transforming response to KU-0063794 in a panel of six CRC cell lines (Fig. S10). Notably, this mTORC inhibitor showed strong inhibitory effects on colony formation and invasive capacities in SLAP-low CRC cell lines—HT29, SW620, DLD1, and LST174T—while having a stimulating effect in SLAP-high CRC cell lines SW480 and HCT116 (Fig. S10C, D). Finally, we investigated whether SLAP downregulation sensitizes CRC to mTORCi in vivo. We turned to the mTORC catalytic inhibitor Torkinib because of its reported effective anti-tumor response in immunodeficient mouse CRC xenograft models [44] and its clinical interest for oncology. We first confirmed that Torkinib inhibited SLAP-dependent growth of tumoroids derived from HCT116 cells, as an ex vivo model of tumorigenesis (Fig. S11). Note that similar results were obtained with the mTORCi AZD2014 (Fig. S11), confirming the mTORC-dependent SLAP effect on this ex vivo cancer model. Next, shCTRL

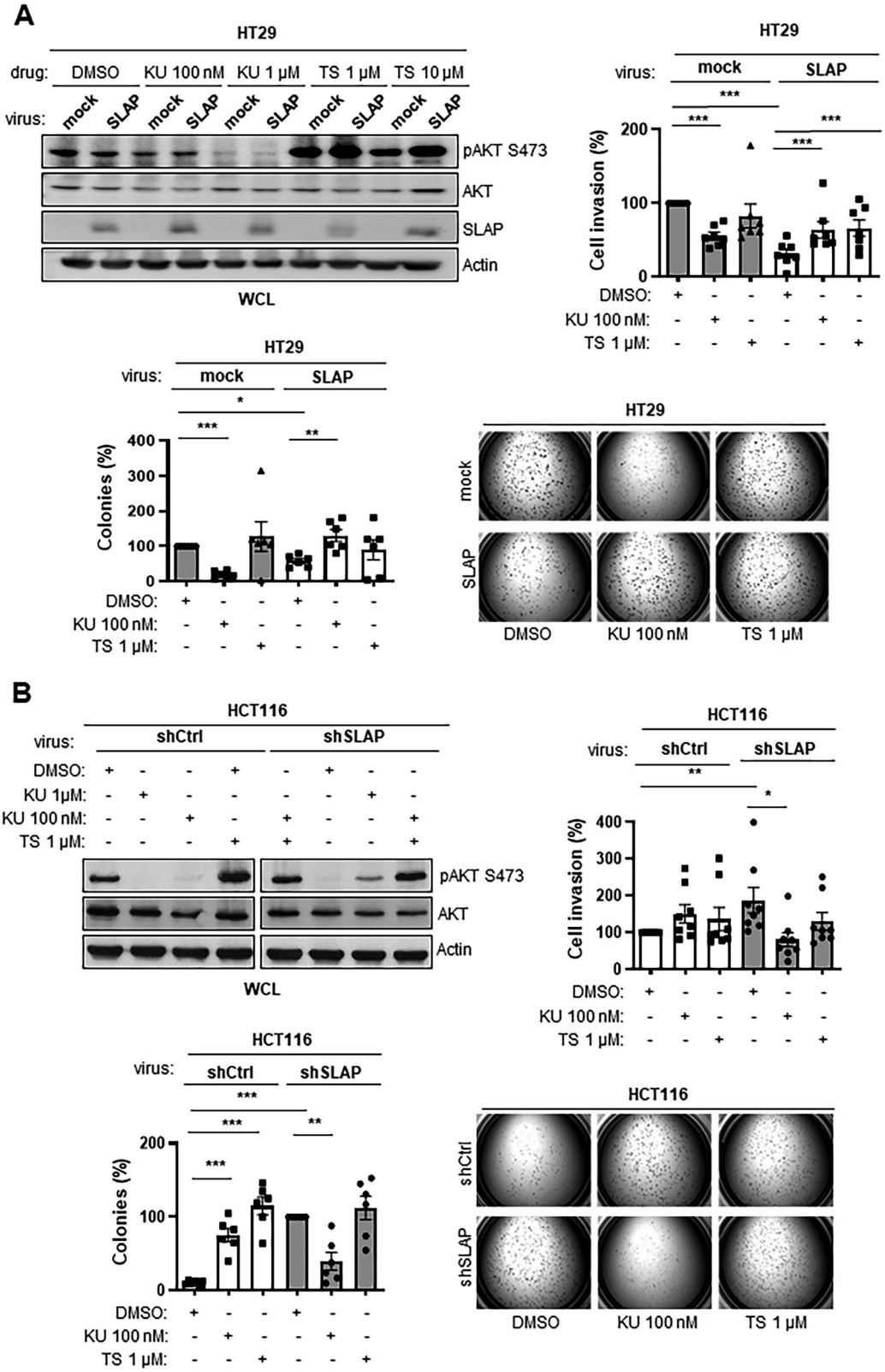

Fig. 7 SLAP influences CRC cell response to mTORCi in vitro. A SLAP-dependent inhibition of HT29 cell transforming properties induced by the mTOR catalytic inhibitor KU-0063794 but not the rapamycin analog Temsilorimus. Top left: WB analysis of the effect of mTOR inhibitors on pS473 AKT levels in HT29 cells expressing or not SLAP. Top right: quantification of cell invasion in Matrigel. Bottom: quantification (left) of colony formation in soft agar (control: 100%) and representative images (right). **B** Enhanced HCT116 cell transforming properties induced by SLAP depletion are sensitive to the mTOR catalytic inhibitor KU-0063794 but not TS. Top left: WB analysis of the effect of mTOR inhibitors on pS473 AKT levels. Top right: quantification of cell invasion in Matrigel (control: 100%). Bottom: quantification (left) of colony formation in soft agar (shRNA SLAP: 100%) and representative images (right). Are shown the mean ± SEM, $n = 3–6$, $^{*}p \leq 0.05$, $^{**}p \leq 0.01$, $^{***}p \leq 0.001$ (Unpaired t-test).

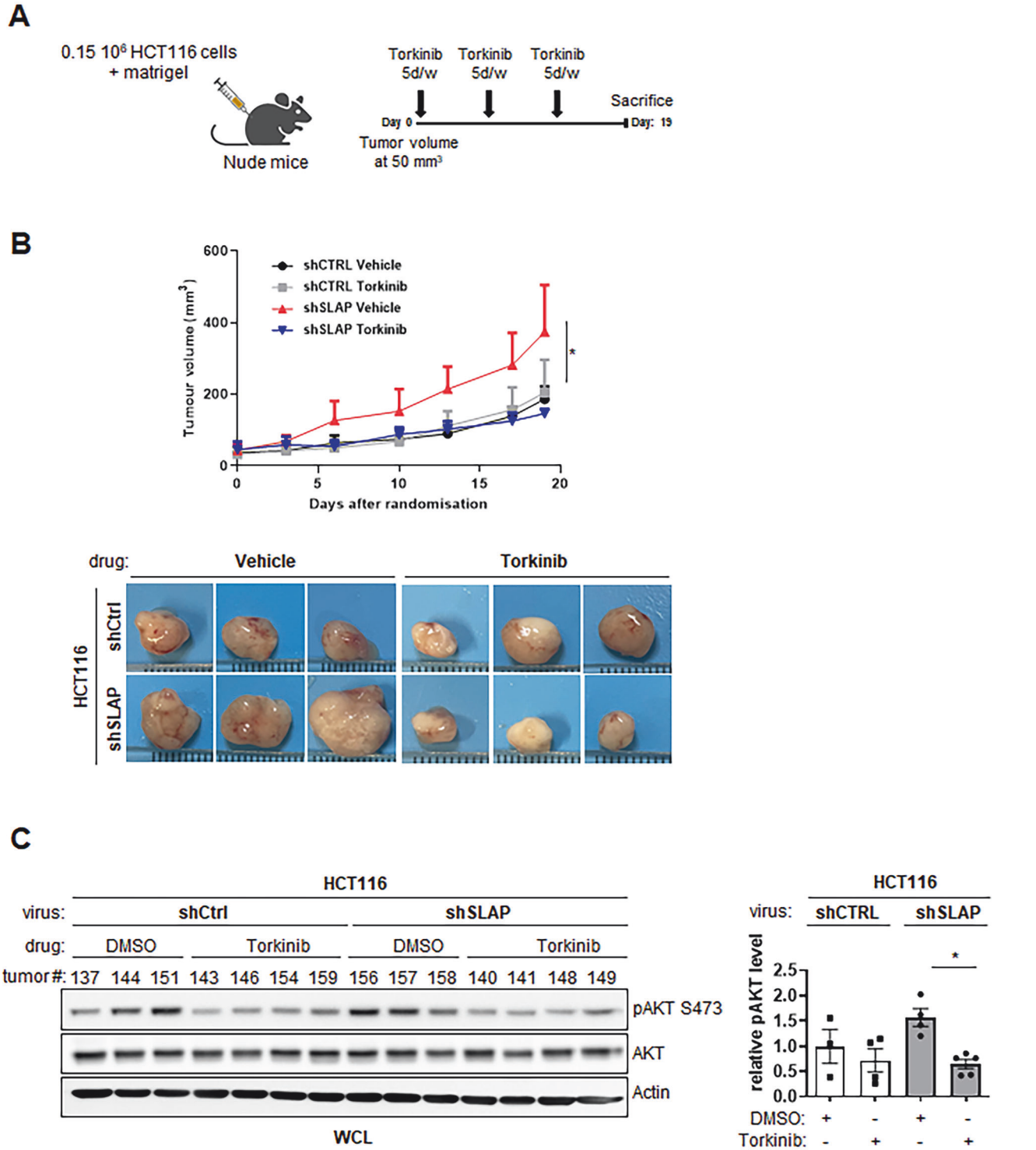

Fig. 8 SLAP influences CRC cell response to mTORCi in vivo. SLAP-dependent anti-tumor activity of the mTORC catalytic inhibitor Torkinib in CRC xenografts. **A** Schematic of mice treatment with mTORCi. **B** Tumor volume induced by control and SLAP-depleted HCT116 cells inoculated into immunodeficient mice and treated daily (5 days/week) with Torkinib and a vehicle as control. Top: tumor growth over time; bottom: representative images of collected tumors. **C** Left: WB analysis of pS473 AKT levels from indicated tumors. Right: corresponding quantification. Are shown the mean ± SEM, $n = 5$ mice/cohort, $^*p \leq 0.05$ (Mann-Whitney test).

or shSLAP HCT116 cells were subcutaneously inoculated into nude mice, followed by daily treatment with Torkinib (or vehicle) when tumors reached a volume of 50 mm^3. Although Torkinib did not affect tumor development in control cells, it abrogated the increased tumor volume induced by SLAP depletion (Fig. 8A, B). This specific anti-tumor effect was associated with a reduction of CRC cell proliferation and increased cell apoptosis (Fig. S12A, B). Similar results were obtained on mTORC2 activity, consistent with the SLAP-dependent mTORC2 tumor function that was targeted by Torkinib (Figs. 8C and S12C). Thus, we conclude that

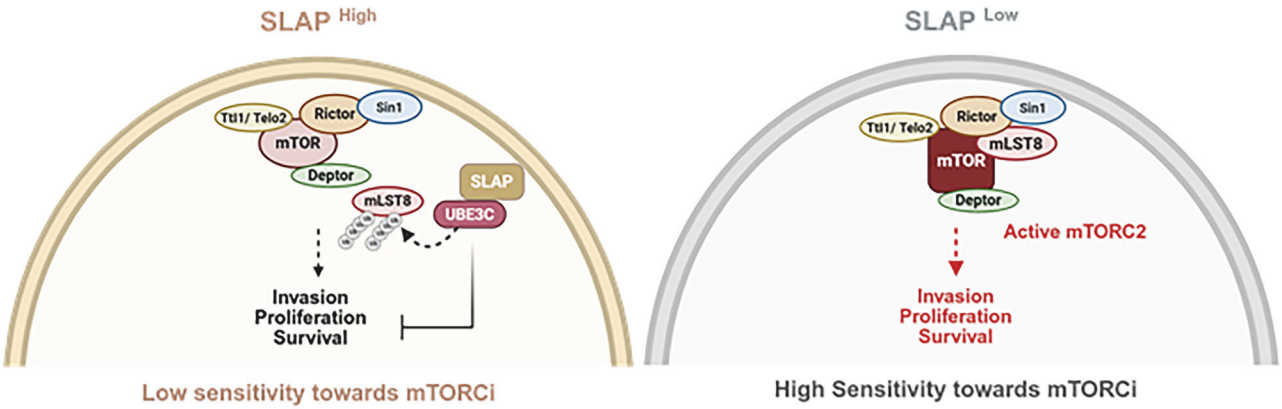

Fig. 9 Proposed model illustrating how SLAP regulates mTORC2 signaling and tumor response to mTORCi in CRC. SLAP promotes UBE3C-mediated non-degradative ubiquitination of mLST8 on K86 and K215, thereby destabilizing mTORC2 integrity and suppressing its oncogenic activity. Differential expression of SLAP defines CRC cell responses to mTOR catalytic inhibitors: SLAP-low tumor cells are sensitive to mTORCi, whereas SLAP-high cells may display paradoxical stimulation.

SLAP acts as an mTORC2 signaling inhibitor in CRC cells and influences the tumor cell response to mTOR catalytic inhibitors (Fig. 9).

DISCUSSION

Tyrosine kinase signaling receptors are under the control of small adaptor proteins, the prototype of which is suppressors of cytokine signaling protein SOCS, which plays an important role in cancer [45]. SLAP belongs to this family and negatively regulates immune cell receptor signaling through proteasomal degradation of specific signaling components [18, 19]. Previously, we reported an unexpected tumor suppressor function of SLAP in the colon and identified the cell adhesion receptor EPHA2 as an important target in this neoplastic process [29].

In the present study, we demonstrate that SLAP additionally acts as an inhibitor of mTORC2 and, through this mechanism, exerts anti-oncogenic effects in CRC. Mechanistically, SLAP, which localizes to the plasma membrane via N-terminal myristoylation [22], may associate with mTORC2 recruited to the membrane by TK/PI3K signaling, particularly through the PH domain of the Sin1 subunit [46]. In this way, SLAP establishes an indirect feedback mechanism that restrains TK-driven oncogenic signaling in CRC. Since EPHA2 has been established as an upstream receptor of AKT signaling [47], our results show that SLAP inhibits an AKT pathway in CRC by targeting multiple nodes of the signaling cascade. In fact, EPHA2 has been reported as both an upstream activator and an AKT substrate, creating a feed-forward loop in cancer signaling [48]. Our findings therefore support a model in which SLAP inhibits mTORC2 activity both through two complementary mechanisms: facilitating complex destabilization and reducing EPHA2/PI3K-dependent mTORC2 activation. The mechanistic details of this regulation, however, remain to be fully defined. While EPHA2 targeting by SLAP requires the SH2 domain and SRC-dependent phosphorylation of EPHA2 at Tyr594, the mode of mTORC2 targeting is less clear, as the complex itself has not been firmly established as a direct TK substrate. Nevertheless, the observed SLAP–mTORC2 association suggests that SLAP-SH2 contributes to this interaction in CRC cells. One possibility is that SLAP engages mTORC2 indirectly when the complex is bound to EPHA2 or to another, yet unidentified, TK receptor. Elucidating the precise molecular mechanism of SLAP-mediated mTORC2 regulation will require further investigation. It should be noted that many of these interactions were identified using overexpression-based approaches, and future studies validating them at endogenous protein levels will be important to confirm their physiological relevance and the overall significance of the findings.

By enabling mTORC2 assembly induced by SLAP downregulation, our study reveals a novel mechanism of mTORC2 dysregulation in cancer. This finding is highly consistent with previous reports showing mTORC2 oncogenic induction upon mLST8 mutation, which facilitates mTORC2 formation [16, 49]. Therefore, dysregulation of complex assembly may be an important mechanism of mTOR oncogenic activation. Mechanistically, ubiquitination of LST8 plays a key role in this molecular process. Our results support a model in which SLAP associates with mTORC2, implicating a SLAP-SH3-dependent mLST8 interaction to recruit UBE3C and facilitate non-degradative LST8 polyubiquitination. While TRAF2 can promote mTORC2 disassembly via K63-linked polyubiquitination of LST8 at K305 and K313 [16], our work suggests that additional UBE3C-dependent polyubiquitination at K86, K215, and possibly K245 also contributes to this process. Structurally, mLST8 forms a 7-bladed β-propeller composed of 5 WD40 domains. These Lys residues are located in WD40 domains 2 and 4, positioned on the outer rim of the propeller, where they directly interact with RICTOR and SIN1 within mTORC2 [13]. These amino acids also play a critical role in stabilizing the C-lobe of the mTOR kinase domain, which is essential for maintaining its active conformation [13]. Consequently, polyubiquitination of these Lys residues by the SLAP–UBE3C complex likely disrupts these protein–protein interactions, shifting mTOR kinase into an inactive state. Supporting this model, mutating Lys 86 and 215 to non-ubiquitinatable residues (arginines) was sufficient to overcome the SLAP-mediated inhibition of mTORC2 integrity. In line with this mechanism, a recent study reveals a similar ubiquitination event at K86 and K261 mediated by the oxidative sensor KEAP1 [49], highlighting the diversity of ubiquitination-dependent mLST8 scaffold inhibition. From this model, several mechanisms of mTORC2 dysregulation in cancer can be proposed, including mLST8 mutations resistant to ubiquitination, as reported in melanoma, or alteration of ubiquitination pathways involved. While oncogenic mLST8 mutations are rare in CRC, mTORC2 overactivation is often associated with the overexpression of multiple complex components, including mTOR and RICTOR [5]. Our findings suggest that overexpression of RICTOR or mLST8 is sufficient to bypass SLAP-dependent mTORC2 inhibition. Thus, we propose that the combination of SLAP downregulation with RICTOR overexpression may contribute to the deregulation of mTORC2 assembly in CRC.

Clinically developed mTORCi have shown variable efficacy in CRC [9–12]. The newly reported mechanism of mTORC2 dysregulation by SLAP downregulation may help predict the therapeutic response to these ATP site inhibitors. For example, overactivation of RTK signaling, such as PI3K or RAS pathways, has been reported

to influence CRC response to mTORCi [9–12]. Our results add SLAP tumor expression as a potential predictor of CRC response to mTORCi. The fact that SLAP controls CRC metastasis in nude mice models and the cell-invasive function of mTORC2 in vitro suggests that SLAP may also regulate the invasive function of mTORC2 in vivo. Whether SLAP expression influences mTORCi activity in metastatic CRC, alone or in combination with chemotherapy, deserves further investigation. Similarly, the PIKK co-chaperones TTI were retrieved from our SLAP proteomic analysis in CRC cells. Whether SLAP also affects PIKK assembly and influences CRC response to PIKK inhibitors is another question to be addressed in the future.

Collectively, our data reveal a central mechanism of mTORC2 oncogenic induction in CRC mediated by dysregulation of complex integrity via downregulation of the tumor suppressor adaptor SLAP, with potential implications in mTORCi-targeted therapy (Fig. 9). By showing that SLAP mediates its signaling function by recruiting diverse ubiquitination factors (i.e. CBL, UBE4A and UBE3C) and possibly additional ones (i.e. LTN1, UBR5, TRIM25…) as revealed by our proteomic analysis, this study sheds light on a more complex signaling mechanism by which SLAP regulates TK signaling receptors than initially reported. Finally, since SLAP is expressed in other cancers (e.g., lung, pancreas, breast and kidney cancer, glioblastoma and leukemia; TCGA data, cancer.gov), this uncovered SLAP activity may also have an important function in these cancers.

DATA AVAILABILITY

The mass spectrometry proteomics data have been deposited to the ProteomeXchange Consortium via the PRIDE [50] partner repository with the dataset identifier PXD068486 and 10.6019/PXD068486. The data that support the findings of this study are available from the corresponding authors upon reasonable request.

REFERENCES

1. Battaglioni S, Benjamin D, Wälchli M, Maier T, Hall MN. mTOR substrate phosphorylation in growth control. Cell. 2022;185:1814–36.
2. Saxton RA, Sabatini DM. mTOR signaling in growth, metabolism, and disease. Cell. 2017;168:960–76.
3. Ragupathi A, Kim C, Jacinto E. The mTORC2 signaling network: targets and cross-talks. Biochem J. 2024;481:45–91.
4. Roulin D, Cerantola Y, Dormond-Meuwly A, Demartines N, Dormond O. Targeting mTORC2 inhibits colon cancer cell proliferation in vitro and tumor formation in vivo. Mol Cancer. 2010;9:57.
5. Gulhati P, Bowen KA, Liu J, Stevens PD, Rychahou PG, Chen M, et al. mTORC1 and mTORC2 regulate EMT, motility, and metastasis of colorectal cancer via RhoA and Rac1 signaling pathways. Cancer Res. 2011;71:3246–56.
6. Sane S, Srinivasan R, Potts RA, Eikanger M, Zagirova D, Freeling J, et al. UBXN2A suppresses the Rictor-mTORC2 signaling pathway, an established tumorigenic pathway in human colorectal cancer. Oncogene. 2023;42:1763–76.
7. Li M, Wu X, Pan Y, Song M, Yang X, Xu J, et al. mTORC2-AKT signaling to PFKFB2 activates glycolysis that enhances stemness and tumorigenicity of intestinal epithelial cells. FASEB J. 2024;38:e23532.
8. Lv G, Wang Q, Lin L, Ye Q, Li X, Zhou Q, et al. mTORC2-driven chromatin cGAS mediates chemoresistance through epigenetic reprogramming in colorectal cancer. Nat Cell Biol. 2024;26:1585–96.
9. Fricke SL, Payne SN, Favreau PF, Kratz JD, Pasch CA, Foley TM, et al. MTORC1/2 inhibition as a therapeutic strategy for PIK3CA mutant cancers. Mol Cancer Ther. 2019;18:346–55.
10. Ng K, Tabernero J, Hwang J, Bajetta E, Sharma S, Del Prete SA, et al. Phase II study of everolimus in patients with metastatic colorectal adenocarcinoma previously treated with bevacizumab-, fluoropyrimidine-, oxaliplatin-, and irinotecan-based regimens. Clin Cancer Res. 2013;19:3987–95.
11. Spindler K-LG, Sorensen MM, Pallisgaard N, Andersen RF, Havelund BM, Ploen J, et al. Phase II trial of temsirolimus alone and in combination with irinotecan for KRAS mutant metastatic colorectal cancer: outcome and results of KRAS mutational analysis in plasma. Acta Oncol. 2013;52:963–70.
12. Di Nicolantonio F, Arena S, Tabernero J, Grosso S, Molinari F, Macarulla T, et al. Deregulation of the PI3K and KRAS signaling pathways in human cancer cells determines their response to everolimus. J Clin Investig. 2010;120:2858–66.
13. Linde-Garelli KY, Rogala KB. Structural mechanisms of the mTOR pathway. Curr Opin Struct Biol. 2023;82:102663.
14. Fernández-Sáiz V, Targosz B-S, Lemeer S, Eichner R, Langer C, Bullinger L, et al. SCFFbxo9 and CK2 direct the cellular response to growth factor withdrawal via Tel2/Tti1 degradation and promote survival in multiple myeloma. Nat Cell Biol. 2013;15:72–81.
15. Turgu B, El-Naggar A, Kogler M, Tortola L, Zhang H-F, Hassan M, et al. The HACE1 E3 ligase mediates RAC1-dependent control of mTOR signaling complexes. EMBO Rep. 2023;24:e56815.
16. Wang B, Jie Z, Joo D, Ordureau A, Liu P, Gan W, et al. TRAF2 and OTUD7B govern a ubiquitin-dependent switch that regulates mTORC2 signalling. Nature. 2017;545:365–9.
17. Wrobel L, Siddiqi FH, Hill SM, Son SM, Karabiyik C, Kim H, et al. mTORC2 assembly is regulated by USP9X-mediated deubiquitination of RICTOR. Cell Rep. 2020;33:108564.
18. Wybenga-Groot LE, McGlade CJ. RTK SLAP down: the emerging role of Src-like adaptor protein as a key player in receptor tyrosine kinase signaling. Cell Signal. 2015;27:267–74.
19. Dragone LL, Shaw LA, Myers MD, Weiss A. SLAP, a regulator of immunoreceptor ubiquitination, signaling, and trafficking. Immunol Rev. 2009;232:218–28.
20. Sosinowski T, Killeen N, Weiss A. The Src-like adaptor protein downregulates the T cell receptor on CD4+CD8+ thymocytes and regulates positive selection. Immunity. 2001;15:457–66.
21. Dragone LL, Myers MD, White C, Sosinowski T, Weiss A. SRC-like adaptor protein regulates B cell development and function. J Immunol. 2006; 176:335–45.
22. Manes G, Bello P, Roche S. Slap negatively regulates Src mitogenic function but does not revert Src-induced cell morphology changes. Mol Cell Biol. 2000;20:3396–406.
23. Roche S, Alonso G, Kazlauskas A, Dixit VM, Courtneidge SA, Pandey A. Src-like adaptor protein (Slap) is a negative regulator of mitogenesis. Curr Biol. 1998;8:975–8.
24. Sirvent A, Leroy C, Boureux A, Simon V, Roche S. The Src-like adaptor protein regulates PDGF-induced actin dorsal ruffles in a c-Cbl-dependent manner. Oncogene. 2008;27:3494–3500.
25. Myers MD, Sosinowski T, Dragone LL, White C, Band H, Gu H, et al. Src-like adaptor protein regulates TCR expression on thymocytes by linking the ubiquitin ligase c-Cbl to the TCR complex. Nat Immunol. 2006;7:57–66.
26. Dragone LL, Myers MD, White C, Gadwal S, Sosinowski T, Gu H, et al. Src-like adaptor protein (SLAP) regulates B cell receptor levels in a c-Cbl-dependent manner. Proc Natl Acad Sci USA. 2006;103:18202–7.
27. Tang J, Sawasdikosol S, Chang J-H, Burakoff SJ. SLAP, a dimeric adapter protein, plays a functional role in T cell receptor signaling. Proc Natl Acad Sci USA. 1999;96:9775–80.
28. Loreto MP, Berry DM, McGlade CJ. Functional cooperation between c-Cbl and Src-like adaptor protein 2 in the negative regulation of T-cell receptor signaling. Mol Cell Biol. 2002;22:4241–55.
29. Naudin C, Sirvent A, Leroy C, Larive R, Simon V, Pannequin J, et al. SLAP displays tumour suppressor functions in colorectal cancer via destabilization of the SRC substrate EPHA2. Nat Commun. 2014;5:3159.
30. Detilleux D, Raynaud P, Pradet-Balade B, Helmlinger D. The TRRAP transcription cofactor represses interferon-stimulated genes in colorectal cancer cells. Elife. 2022;11:e69705.
31. Aponte E, Lafitte M, Sirvent A, Simon V, Barbery M, Fourgous E, et al. Regulation of Src tumor activity by its N-terminal intrinsically disordered region. Oncogene. 2022;41:960–70.
32. Sarbassov DD, Ali SM, Kim D-H, Guertin DA, Latek RR, Erdjument-Bromage H, et al. Rictor, a novel binding partner of mTOR, defines a rapamycin-insensitive and raptor-independent pathway that regulates the cytoskeleton. Curr Biol. 2004;14:1296–302.
33. Ounoughene Y, Fourgous E, Boublik Y, Saland E, Guiraud N, Recher C, et al. SHED-dependent oncogenic signaling of the PEAK3 pseudo-kinase. Cancers. 2021;13:6344.
34. Wybenga-Groot LE, McGlade CJ. Crystal structure of Src-like adaptor protein 2 reveals close association of SH3 and SH2 domains through β-sheet formation. Cell Signal. 2013;25:2702–8.
35. Michel MA, Elliott PR, Swatek KN, Simicek M, Pruneda JN, Wagstaff JL, et al. Assembly and specific recognition of k29- and k33-linked polyubiquitin. Mol Cell. 2015;58:95–109.
36. Sun C, Chen Y, Gu Q, Fu Y, Wang Y, Liu C, et al. UBE3C tunes autophagy via ATG4B ubiquitination. Autophagy. 2024;20:645–58.
37. Chen Y-H, Huang T-Y, Lin Y-T, Lin S-Y, Li W-H, Hsiao H-J, et al. VPS34 K29/K48 branched ubiquitination governed by UBE3C and TRABID regulates autophagy, proteostasis and liver metabolism. Nat Commun. 2021;12:1322.

38. Meng K, Yang J, Xue J, Lv J, Zhu P, Shi L, et al. A host E3 ubiquitin ligase regulates Salmonella virulence by targeting an SPI-2 effector involved in SIF biogenesis. mLife. 2023;2:141–58.
39. Di Rienzo M, Antonioli M, Fusco C, Liu Y, Mari M, Orhon I, et al. Autophagy induction in atrophic muscle cells requires ULK1 activation by TRIM32 through unanchored K63-linked polyubiquitin chains. Sci Adv. 2019;5:eaau8857.
40. Glaviano A, Foo ASC, Lam HY, Yap KCH, Jacot W, Jones RH, et al. PI3K/AKT/mTOR signaling transduction pathway and targeted therapies in cancer. Mol Cancer. 2023;22:138.
41. García-Martínez JM, Moran J, Clarke RG, Gray A, Cosulich SC, Chresta CM, et al. Ku-0063794 is a specific inhibitor of the mammalian target of rapamycin (mTOR). Biochem J. 2009;421:29–42.
42. Blaser B, Waselle L, Dormond-Meuwly A, Dufour M, Roulin D, Demartines N, et al. Antitumor activities of ATP-competitive inhibitors of mTOR in colon cancer cells. BMC Cancer. 2012;12:86.
43. Rashid MM, Lee H, Jung BH. Evaluation of the antitumor effects of PP242 in a colon cancer xenograft mouse model using comprehensive metabolomics and lipidomics. Sci Rep. 2020;10:17523.
44. Zhang J, Jiang W, Liu W, Wu J-J, Song L, Cheng J-X, et al. Effective targeting of colorectal cancer cells using TORC1/2 kinase inhibitors in vitro and in vivo. Future Oncol. 2016;12:515–24.
45. Naudin C, Chevalier C, Roche S. The role of small adaptor proteins in the control of oncogenic signalingr driven by tyrosine kinases in human cancer. Oncotarget. 2016;7:11033–55.
46. Liu P, Gan W, Chin YR, Ogura K, Guo J, Zhang J, et al. PtdIns(3,4,5)P3-dependent activation of the mTORC2 kinase complex. Cancer Discov. 2015;5:1194–209.
47. Wilson K, Shiuan E, Brantley-Sieders DM. Oncogenic functions and therapeutic targeting of EphA2 in cancer. Oncogene. 2021;40:2483–95.
48. Miao H, Li DQ, Mukherjee A, Guo H, Petty A, Cutter J, et al. EphA2 mediates ligand-dependent inhibition and ligand-independent promotion of cell migration and invasion via a reciprocal regulatory loop with Akt. Cancer Cell. 2009;16 https://doi.org/10.1016/j.ccr.2009.04.009.
49. Chen Y, Jiao D, He H, Sun H, Liu Y, Shi Q, et al. Disruption of the Keap1-mTORC2 axis by cancer-derived Keap1/mLST8 mutations leads to oncogenic mTORC2-AKT activation. Redox Biol. 2023;67:102872.
50. Perez-Riverol Y, Bandla C, Kundu DJ, Kamatchinathan S, Bai J, Hewapathirana S, et al. The PRIDE database at 20 years: 2025 update. Nucleic Acids Res. 2025;53:D543–D553.

ACKNOWLEDGEMENTS

We acknowledge Montpellier Biocampus facilities: Montpellier Ressources Imagerie (MRI) platform, the histology and animal experimentation platforms RHEM and RAM, the PCEA and IGMM mouse facilities ZEFI, and the Proteomic Core Platform of FPP for proteomic analyses. This work was supported by La Ligue Nationale Contre le Cancer (LNCC), La Foundation pour la Recherche Médicale, Montpellier SIRIC Grant «INCa-DGOS-Inserm 6045», CNRS, and the University of Montpellier. MRI platform, a member of the national infrastructure France-BioImaging (https://ror.org/01y7vt929), is supported by the French National Research Agency (ANR-24-INBS-0005 FBI BIOGEN). RHEM facility supported by SIRIC Montpellier Cancer Grant INCa_Inserm_DGOS_12553, the European regional development foundation and the Occitanie region (FEDER-FSE 2014-2020 Languedoc Roussillon), la Ligue Contre le Cancer for processing our animal tissues and histology techniques. RM and DN were supported by the LNCC, ARC and Montpellier University. SR is an INSERM investigator. We thank Daniel FISHER, Dominique HELMLINGER, Zouheir HOUHOU, Dimitris XIRODIMAS, and our colleagues for the technical support and fruitful discussion on the study.

AUTHOR CONTRIBUTIONS

All authors contributed extensively to the work presented in this paper. Experimental analysis and Data acquisition: RM, DN, FC, CN, GG, BF, KE, VS, YB, JN and AS. MS analysis: SU. Project supervision: SR and AS. Funding acquisition and Writing of the paper: SR.

FUNDING

This work was supported by La Ligue Nationale Contre le Cancer (LNCC) through the Labelling Team programs 2017 and 2020, and by La Fondation pour la Recherche Médicale through the Labelling Team program 2023. Additional support was provided by the Montpellier SIRIC grant "INCa-DGOS-Inserm 6045," CNRS, and the University of Montpellier. The MRI platform, a member of the national infrastructure France-BioImaging (https://ror.org/01y7vt929), is supported by the French National Research Agency (ANR-24-INBS-0005 FBI BIOGEN). The RHEM facility is supported by the SIRIC Montpellier Cancer grant INCa_Inserm_DGOS_12553, the European Regional Development Fund and the Occitanie region (FEDER-FSE 2014–2020 Languedoc-Roussillon), and La Ligue Contre le Cancer for processing animal tissues and histology. RM was supported by the Association pour la Recherche contre le Cancer (ARC), and DN was supported by LNCC.

COMPETING INTERESTS

The authors declare no competing interests.

ETHICS

Animal experiments were performed in compliance with the French guidelines for experimental animal studies (Direction des services vétérinaires, ministère de l'agriculture, France, APAFIS #35916-2022031511382008 v6, local animal house agreement number F3417216).

ADDITIONAL INFORMATION

Supplementary information The online version contains supplementary material available at https://doi.org/10.1038/s41418-025-01633-1.

Correspondence and requests for materials should be addressed to Serge Roche or Audrey Sirvent.

Reprints and permission information is available at http://www.nature.com/reprints

Publisher's note Springer Nature remains neutral with regard to jurisdictional claims in published maps and institutional affiliations.